

Dynamic Power Splitting for SWIPT with Nonlinear Energy Harvesting in Ergodic Fading Channel

Jae-Mo Kang, Chang-Jae Chun, Il-Min Kim, *Senior Member, IEEE*, and Dong In Kim, *Senior Member, IEEE*

arXiv:1804.07398v1 [cs.IT] 19 Apr 2018

Abstract—We study the dynamic power splitting for simultaneous wireless information and power transfer (SWIPT) in the ergodic fading channel. Considering the nonlinearity of practical energy harvesting circuits, we adopt the realistic nonlinear energy harvesting (EH) model rather than the idealistic linear EH model. To characterize the optimal rate-energy (R-E) tradeoff, we consider the problem of maximizing the R-E region, which is nonconvex. We solve this challenging problem for two different cases of the channel state information (CSI): (i) when the CSI is known only at the receiver (CSIR case) and (ii) when the CSI is known at both the transmitter and the receiver (CSIT case). First, for the case of CSIR, we develop the optimal dynamic power splitting scheme. To address the complexity issue of the optimal scheme, we also propose a suboptimal scheme with low complexity. Comparing the proposed schemes to the existing schemes, we provide various useful and interesting insights into the dynamic power splitting for the nonlinear EH. Second, we present the optimal and suboptimal schemes for the case of CSIT, and we obtain further insights. Numerical results demonstrate that the proposed schemes significantly outperform the existing schemes and the proposed suboptimal scheme works very close to the optimal scheme at a much lower complexity.

Index Terms—Dynamic power splitting, nonlinear energy harvesting, power allocation, rate-energy tradeoff, simultaneous wireless information and power transfer.

I. INTRODUCTION

As a promising technology for future energy-constrained networks, simultaneous wireless information and power transfer (SWIPT) using radio frequency (RF) signals has recently drawn an upsurge of research interest in the literature [1]. A practical limitation for the SWIPT is that with the current circuit technology, it is difficult to carry out both information decoding (ID) and energy harvesting (EH) at the same time from the same received RF signal [2], [3]. Thus, in the practical SWIPT system, there exists a tradeoff between the amount of information transfer and the amount of energy transfer, which is called the rate-energy (R-E) tradeoff [2], [3]. To characterize and understand the fundamental performance of the SWIPT system, analyzing the R-E tradeoff is essential and crucial. In the literature, the R-E tradeoff for the SWIPT has been studied under different fading environments, e.g., in the additive white Gaussian noise (AWGN) channel without fading [2]–[7] and in the fading channel [10]–[14]. Unlike the AWGN channel, in the fading channel, the received RF power

J.-M. Kang, C.-J. Chun, and I.-M. Kim are with the Department of Electrical and Computer Engineering, Queen's University, Kingston, ON K7L 3N6, Canada (e-mail: jaemo.kang@queensu.ca; changjae.chun@queensu.ca; ilmin.kim@queensu.ca).

D. I. Kim is with the School of Information and Communication Engineering, Sungkyunkwan University (SKKU), Suwon, 440-746, South Korea (e-mail: dikim@skku.ac.kr).

variation due to the fading fluctuation can be effectively and opportunistically utilized for the SWIPT. For this purpose, two different schemes were investigated, namely, the mode switching [8]–[13] and the dynamic power splitting [14]. In this paper, we study the R-E tradeoff of the dynamic power splitting in the fading channel.

In [14], the optimal dynamic power splitting scheme was developed in the sense of the R-E tradeoff. However, in [14], it was assumed that the amount of energy harvested by the EH circuit is linearly proportional to the received RF power, namely, the linear EH model. This idealistic (i.e., linearity) assumption is valid only when the energy conversion efficiency of the EH circuitry is the same (i.e., constant) for all the received RF power levels. However, as studied in the very recent literature [6]–[9], [16]–[26], the linear EH model is overly idealistic and impractical because the linearity assumption does not hold in practice. Specifically, as validated in many experimental results [27]–[29], the energy conversion efficiency of the practical EH circuit becomes different (not constant) depending on the received RF power level. Also, as analyzed in [16]–[19], the energy conversion efficiency of the actual EH circuit (or rectifier) is a nonlinear function of the received RF signal (i.e., power and shape) due to various causes of nonlinearity, e.g., nonlinearity of the diode. In practice, therefore, the amount of harvested energy is clearly a nonlinear function of the received power. Unfortunately, the linear EH model cannot accurately model the nonlinear behavior of the practical EH circuit [6]–[9], [16]–[26], which may incur severe mismatch or inaccuracy in the practical system. To overcome the limitations of the linear model, one should address the practical issue of nonlinear EH.

In [8], [9], the mode switching scheme was studied for the realistic scenario of nonlinear EH. In these works, an important and crucial conclusion was made: the mode switching scheme developed for the linear EH is no longer optimal for the nonlinear EH, because the linear and nonlinear EH models are practically and mathematically different. From this result, one can expect that the existing dynamic power splitting scheme developed in [14] for the linear EH might not work well or might lead to misleading/wrong conclusion for the nonlinear EH. In addition, none of the existing mode switching schemes developed in [8], [9] for the nonlinear EH are truly optimal in the sense of achieving the ultimate R-E tradeoff performance of the SWIPT system, because the mode switching can be considered as a special and simplified case of the dynamic power splitting [14], meaning that the dynamic power splitting generally yields better performance than the mode switching. To achieve the theoretically best performance of the SWIPT

system in the fading channel, the corresponding optimal dynamic power splitting scheme must be studied. To the best of our knowledge, for the SWIPT system with nonlinear EH in the ergodic fading channel, the optimal dynamic power splitting scheme has not been studied in the literature. This motivated our work.

In this paper, we study the dynamic power splitting for the SWIPT system with nonlinear EH in the ergodic fading channel. For analysis, we adopt a realistic nonlinear EH model developed in [24]–[26], which was shown to accurately match the experimental results reported in the literature [23]. Using this nonlinear model, to characterize the optimal R-E tradeoff, we formulate the optimal dynamic power splitting problem to maximize the average achievable rate under the constraints on the average harvested energy and the average transmit power, which is a nonconvex problem. We solve this challenging problem for two different cases of the channel state information (CSI): (i) when the CSI is known only at the receiver (the CSIR case) and (ii) when the CSI is known at both the transmitter and the receiver (the CSIT case). The main contributions of this paper are three-fold as follows:

- In the case of CSIR, we develop the optimal power splitting scheme for the SWIPT system with nonlinear EH. Also, to address the complexity issue of the optimal scheme, we propose a suboptimal scheme with low complexity, which is shown to be asymptotically optimal in the low signal-to-noise ratio (SNR) regime.
- As a different case from the CSIR case, we further study the CSIT case. In this case, we develop the optimal and suboptimal power splitting schemes. We also establish the asymptotically optimality of the proposed suboptimal scheme in the low SNR regime.
- Through comparisons between the proposed and existing schemes, we provide various useful and interesting insights into the dynamic power splitting for the nonlinear EH.

This paper is organized as follows. In Section II, the system model is described and the problem is formulated. In Sections III and IV, we develop the optimal and suboptimal dynamic power splitting schemes for the cases of CSIR and CSIT, respectively. Section V presents the numerical results and Section VI concludes the paper.

II. SYSTEM MODEL AND PROBLEM FORMULATION

We consider a point-to-point SWIPT system with a transmitter and a receiver, each of which is equipped with a single antenna. It is assumed that the channel between the transmitter and receiver remains constant during one coherent fading block of duration T , but it varies from one block to another block independently [15]. We assume the ergodic fading channel: a codeword spans over many fading blocks,¹ i.e., $N \rightarrow \infty$, where N denotes the number of fading blocks.¹

The dynamic power splitting scheme is adopted at the receiver. At a particular fading state ν , the received power

¹ In this paper, the number N of fading blocks is assumed to be infinite for theoretical analysis. However, in practice, N should be sufficiently large, but finite [30]. The practical range of N (enough to justify the ergodicity) is given by $N \geq \mathcal{O}(10^3)$, i.e., the order of 10^3 or more [15].

is dynamically split with a power splitting ratio $0 \leq \rho_\nu \leq 1$. Specifically, the ρ_ν portion of the received power is used for EH and the remaining $(1 - \rho_\nu)$ portion of the received power is used for ID. Let P_ν denotes the transmit power at the fading state ν . Then the average achievable rate over the fading blocks is given by $\mathbb{E}[R_\nu(P_\nu, \rho_\nu)]$ [15], where $\mathbb{E}[\cdot]$ denotes the expectation operation taken over the fading process and

$$R_\nu(P_\nu, \rho_\nu) = \log_2 \left(1 + \frac{(1 - \rho_\nu)h_\nu P_\nu}{\sigma^2} \right). \quad (1)$$

Also, h_ν denotes the channel power gain at the fading state ν , and σ^2 the variance of the additive noise. In the next subsection, the amount of harvested energy will be discussed in detail.

A. Linear and Nonlinear Energy Harvesting

In the existing works including [10]–[13], [14], the linear EH model was adopted. In the linear EH model, at the fading state ν , the amount of harvested energy is modeled as where

$$Q_\nu^L(P_\nu, \rho_\nu) = \zeta \rho_\nu h_\nu P_\nu T. \quad (2)$$

In (2), $0 < \zeta \leq 1$ denotes the energy conversion efficiency, which is assumed to be a constant and be independent of the received RF power $h_\nu P_\nu$. However, the energy conversion efficiency of the actual EH circuit is different (not constant) over the different received RF power levels, as studied in [16]–[19] and validated in the experimental results [27]–[29]. In practice, the amount of harvested energy of the actual EH circuit increases *nonlinearly* with the received RF power. Specifically, in the low RF power level, the energy conversion efficiency is very small (close to zero) due to the turn-on voltage of the diode; in the middle RF power level, the efficiency is large (about 0.7 at the RF frequency of 915 MHz [27]) because the diode works in the linear region; and in the high RF power level, the efficiency is again very small (close to zero) due to the reverse breakdown of the diode. Unfortunately, the simplistic linear model of (2) cannot accurately model the nonlinearity of the practical EH circuits, and thus, it is never realistic in practical systems.

In order to address the critical limits of the linear EH model and to accurately model the nonlinear behavior of the actual EH circuit, several realistic nonlinear EH models were developed and studied in the recent literature [16]–[26]. In [16]–[19], the nonlinearity of the rectifier was modeled based on the nonlinearity of the diode characteristic equation. On the other hand, in [23]–[26], the nonlinearity of the energy conversion efficiency was modeled based on nonlinear functions. Among the various nonlinear models, the nonlinear model developed in [24]–[26] was shown to accurately match the experimental results, e.g., see [23, Figs. 2, 3, and Table I], [24, Fig. 2]. In this paper, for accuracy, validity, and practicality of the analysis with useful insights, we adopt the realistic nonlinear EH model of [24]–[26]. Note that the analysis presented in this paper can be extended to the other nonlinear models considered in [17]–[23]. In the adopted nonlinear model, the amount of the

harvested energy is modeled using the logistic (or sigmoid) function, i.e., S-shaped curve, as follows [24]–[26]: where

$$Q_{\nu}^{\text{NL}}(P_{\nu}, \rho_{\nu}) = \frac{P_s T [\Psi_{\nu}(P_{\nu}, \rho_{\nu}) - \Omega]}{1 - \Omega} \quad (3)$$

where $\Omega = \frac{1}{1+e^{ab}}$ is a constant to ensure the zero-input zero-output response and $\Psi_{\nu}(P_{\nu}, \rho_{\nu})$ is the logistic function given by

$$\Psi_{\nu}(P_{\nu}, \rho_{\nu}) = \frac{1}{1 + e^{-a(\rho_{\nu} h_{\nu} P_{\nu} - b)}}. \quad (4)$$

In (3), P_s denotes the maximum amount of harvested power when the EH circuit is saturated. Also, a and b are positive constants related to the circuit specification. Given the EH circuit, the parameters P_s , a , and b can be determined by the curve fitting. In what follows, therefore, those parameters are assumed to be given.

B. Problem Formulation

In this paper, using the realistic nonlinear model $Q_{\nu}^{\text{NL}}(\cdot)$, we aim to develop the optimal dynamic power splitting scheme in the sense of the R-E tradeoff. We consider two different cases of the CSI availability: (i) the CSIR case and (ii) the CSIT case. In the following, the optimization problems for these two cases are formulated.

1) *CSIR Case*: In this case, the CSI is known at the receiver, but unknown at the transmitter. Over the duration of a codeword, the receiver dynamically splits the received power using the power splitting ratios $0 \leq \rho_{\nu} \leq 1, \forall \nu$. On the other hand, the transmit power is fixed, i.e., $P_{\nu} = P, \forall \nu$. In the case of CSIR, the R-E region is given by

$$\mathcal{C}_{\text{CSIR}}^{\text{NL}} = \bigcup_{0 \leq \rho_{\nu} \leq 1, \forall \nu} \left\{ (R, Q) : Q \leq \mathbb{E}[Q_{\nu}^{\text{NL}}(P, \rho_{\nu})], R \leq \mathbb{E}[R_{\nu}(P, \rho_{\nu})] \right\}, \quad (5)$$

which contains all pairs of the average achievable rate and the average harvested energy. To achieve the optimal R-E tradeoff with CSIR, we have to maximize the R-E region $\mathcal{C}_{\text{CSIR}}^{\text{NL}}$ of (5) by optimizing the power splitting ratios $\{\rho_{\nu}\}$, which can be formulated as follows:

$$(P1) : \max_{0 \leq \rho_{\nu} \leq 1, \forall \nu} \mathbb{E}[R_{\nu}(P, \rho_{\nu})] \quad (6a)$$

$$\text{s.t. } \mathbb{E}[Q_{\nu}^{\text{NL}}(P, \rho_{\nu})] \geq Q. \quad (6b)$$

In (P1), $0 \leq Q \leq Q_{\text{max}}^{\text{CSIR}}$ denotes a threshold for the average harvested energy, where $Q_{\text{max}}^{\text{CSIR}} = \mathbb{E}[Q_{\nu}^{\text{NL}}(P, 1)]$ is the maximum amount of harvested energy achieved with $\rho_{\nu} = 1, \forall \nu$.

2) *CSIT Case*: Different from the CSIR case, we also study the CSIT case assuming that the CSI feedback from the receiver to the transmitter is available. In this case, the CSI is known at both the transmitter and the receiver. Over the duration of a codeword, the receiver dynamically splits the received power using the power splitting ratios $0 \leq \rho_{\nu} \leq 1, \forall \nu$. At the same time, the transmitter dynamically adapts the transmit power $P_{\nu}, \forall \nu$, under the long-term power constraint $\mathbb{E}[P_{\nu}] \leq P_{\text{avg}}$ and the short-term power constraint $P_{\nu} \leq$

$P_{\text{max}}, \forall \nu$, where P_{max} and P_{avg} denote the long-term and short-term power thresholds, respectively. In the case of CSIT, the R-E region is given by

$$\mathcal{C}_{\text{CSIT}}^{\text{NL}} = \bigcup_{\substack{0 \leq \rho_{\nu} \leq 1, \forall \nu, \\ 0 \leq P_{\nu} \leq P_{\text{max}}, \forall \nu, \\ \mathbb{E}[P_{\nu}] \leq P_{\text{avg}}}} \left\{ (R, Q) : Q \leq \mathbb{E}[Q_{\nu}^{\text{NL}}(P_{\nu}, \rho_{\nu})], R \leq \mathbb{E}[R_{\nu}(P_{\nu}, \rho_{\nu})] \right\}. \quad (7)$$

To achieve the optimal R-E tradeoff with CSIT, we have to maximize the R-E region $\mathcal{C}_{\text{CSIT}}^{\text{NL}}$ of (7) by jointly optimizing the transmit power $\{P_{\nu}\}$ and the power splitting ratios $\{\rho_{\nu}\}$, which can be formulated as follows:

$$(P2) : \max_{\substack{0 \leq \rho_{\nu} \leq 1, \forall \nu, \\ 0 \leq P_{\nu} \leq P_{\text{max}}, \forall \nu}} \mathbb{E}[R_{\nu}(P_{\nu}, \rho_{\nu})] \quad (8a)$$

$$\text{s.t. } \mathbb{E}[Q_{\nu}^{\text{NL}}(P_{\nu}, \rho_{\nu})] \geq Q, \quad (8b)$$

$$\mathbb{E}[P_{\nu}] \leq P_{\text{avg}}. \quad (8c)$$

In (P2), $0 \leq Q \leq Q_{\text{max}}^{\text{CSIT}}$ is the threshold for the average harvested energy, where $Q_{\text{max}}^{\text{CSIT}} = \max_{0 \leq P_{\nu} \leq P_{\text{max}}, \forall \nu} \mathbb{E}[Q_{\nu}^{\text{NL}}(P_{\nu}, 1)]$, which can be determined based on the result of [9, Theorem 1]. In (P2), to avoid any trivial solution for the power allocation, we assume that $P_{\text{max}} > P_{\text{avg}}$.

The problems (P1) and (P2) are nonconvex because the objective functions and the constraints are nonconvex. Also, the objective and constraint functions of (P1) and (P2) involve the expectations over the fading process, of which closed-form expressions are very difficult to obtain. Thus, it is generally very challenging to tackle the problems (P1) and (P2). One might try to use the exhaustive searching to find the solution. However, this approach appears to be practically infeasible due to extremely high computational complexity that grows exponentially with the (large) number N of fading blocks. Also, such approach does not provide any insight.

Remark 1: In [14], the dynamic power splitting problem for the linear EH model $Q_{\nu}^{\text{L}}(\cdot)$ was studied in both cases of CSIR and CSIT. However, the solution of [14] is no longer optimal for the nonlinear EH model $Q_{\nu}^{\text{NL}}(\cdot)$, because the linear and nonlinear EH models are mathematically and practically very different [8], [9]. In [8] and [9], the mode switching problem for the nonlinear EH model $Q_{\nu}^{\text{NL}}(\cdot)$ was studied in the cases of CSIR and CSIT, respectively. However, in the mode switching considered in [8], [9], the power splitting ratio was restricted to be binary, i.e., $\rho_{\nu} \in \{0, 1\}, \forall \nu$. On the other hand, in the dynamic power splitting considered in this paper, the power splitting ratio can take any continuous value between zero and one, i.e., $0 \leq \rho_{\nu} \leq 1, \forall \nu$. Therefore, the problems studied in [8] and [9] are only the special cases of (P1) and (P2), respectively, and thus, the solutions of [8] and [9] are no longer optimal to (P1) and (P2), respectively. Clearly, the problems (P1) and (P2) are much more challenging than the problems in [8] and [9], respectively, and the extensions of [8] and [9] are never straightforward. ■

Remark 2: In [6] and [7], for the SWIPT system with nonlinear EH, the dynamic power splitting problem was studied over the quasi-static fading channel, in which the duration

of each codeword is not longer than the duration of a single fading block, and thus, one or more codewords span over a single fading block. Unlike [6] and [7], in this paper, we consider the *ergodic* fading channel, in which the duration of each codeword is much longer than the duration of a fading block, and thus, each codeword spans over many fading blocks. Due to the channel variation within each codeword in ergodic fading, the problems (P1) and (P2) are much more challenging than the problems in [6] and [7], respectively, and the extensions of [6] and [7] are never straightforward. The further differences between this paper and the works [6], [7] are that in [6], the power allocation problem at the transmitter was not considered and, in [7], the impact of nonlinearity at the small RF power level was not considered. ■

In order to address all of the shortcomings in the literature, we present the optimal solutions and low complexity suboptimal solutions to (P1) and (P2) in the next two sections.

III. DYNAMIC POWER SPLITTING FOR NONLINEAR EH WITH CSIR

In this section, we first derive the optimal solution to (P1). Then we propose a suboptimal solution to (P1) with low complexity. Finally, we compare the proposed scheme to the existing schemes.

A. Optimal Solution to (P1)

In order to solve the problem (P1) optimally and efficiently, we exploit the time-sharing condition proposed in [30]. To this end, in the following, we first define the time-sharing condition for (P1).

Definition 1 ([30, Definition 1]): Let $\{\rho_{x,\nu}\}$ and $\{\rho_{y,\nu}\}$ denote the optimal solutions to the problem (P1) when $Q = Q_x$ and $Q = Q_y$, respectively. It is said that (P1) satisfies the *time-sharing* condition (or time-sharing property) if there exists a feasible solution $\{\rho_{z,\nu}\}$ such that $\mathbb{E}[Q_{\nu}^{\text{NL}}(P, \rho_{z,\nu})] \geq \theta Q_x + (1 - \theta)Q_y$ and $\mathbb{E}[R_{\nu}(P, \rho_{z,\nu})] \geq \theta \mathbb{E}[R_{\nu}(P, \rho_{x,\nu})] + (1 - \theta) \mathbb{E}[R_{\nu}(P, \rho_{y,\nu})]$ for any $0 \leq \theta \leq 1$. ■

A useful fact is that if an optimization problem satisfies the time-sharing condition, then the strong duality always holds, i.e., the duality gap is always zero, regardless of the convexity of the problem [30, Theorem 1]. In the following, we establish the time-sharing property of (P1).

Lemma 1: In the problem (P1), the time-sharing condition is satisfied.

Proof: See Appendix A. ■

By Lemma 1, it is possible to find the optimal solution to (P1) based on the Lagrange duality method. However, even if the Lagrange duality method can be used, it is still difficult to obtain the solution to (P1) because the Lagrangian is a nonconvex function of $\{\rho_{\nu}\}$. To overcome this difficulty, we take the following approach: we first classify the conditions of the channel power gain h_{ν} into the five mutually exclusive cases, and then, we derive the optimal solution in each case. Taking this approach, we have the following result.

Theorem 1: The solution to (P1) is given by (9) (shown at the top of the next page), where $\rho_{o,\nu}^{\text{NL}}$ is the root of the following equation:

$$\lambda^{\text{NL}} \Psi_{\nu}(P, x) (1 - \Psi_{\nu}(P, x)) = \frac{1 - \Omega}{P_s T a ((1 - x) h_{\nu} P + \sigma^2)} \quad (12)$$

over $x \in \left(\frac{b}{h_{\nu} P}, 1\right)$. Also, the Cases 1–5 are given by (10) (shown at the top of the next page), where $f(x) = \frac{e^{-a(xP-b)}}{(1+e^{-a(xP-b)})^2}$, $g(x) = \frac{1-\Omega}{P_s T a (xP+\sigma^2)}$, and $\gamma(x) = \frac{1-\Omega}{P_s T a (\max\{xP-b, 0\}+\sigma^2)}$. The constant $\lambda^{\text{NL}} > 0$ is chosen to satisfy $\mathbb{E}[Q_{\nu}^{\text{NL}}(P, \rho_{\nu}^{\text{NL}})] = Q$.

Proof: See Appendix B. ■

From Theorem 1, the optimal solution to (P1) can be computed efficiently. Specifically, at each fading state ν , one can determine the optimal power splitting ratio ρ_{ν}^{NL} according to (9) by simply checking which case the channel power gain h_{ν} falls into (through the functions $f(\cdot)$, $g(\cdot)$, and $\gamma(\cdot)$). In the proposed solution, only the positive scalars λ^{NL} and $\{\rho_{o,\nu}\}$ need to be computed numerically by solving the nonlinear equations of $\mathbb{E}[Q_{\nu}^{\text{NL}}(P, \rho_{\nu}^{\text{NL}})] = Q$ and (12), respectively. Since $\mathbb{E}[Q_{\nu}^{\text{NL}}(P, \rho_{\nu}^{\text{NL}})]$ is monotonic in λ^{NL} , the value of λ^{NL} can be found efficiently via the subgradient method as follows [30]: $\lambda^{i+1} = \max \{ \lambda^i - s^i (\mathbb{E}[Q_{\nu}^{\text{NL}}(P, \rho_{\nu}^{\text{NL}})] - Q), 0 \}$, where i denotes the iteration number, λ^i the value of λ^{NL} at the i th iteration, and $s^i > 0$ the step size at the i th iteration. The complexity of finding λ^{NL} is given by $\mathcal{O}(1^2) = \mathcal{O}(1)$ [31]. Also, the value of $\rho_{o,\nu}^{\text{NL}}$ can be found efficiently using the one-dimensional searching, e.g., the bisection method, of which complexity is at most $\mathcal{O}(K)$ [31], where the parameter $K > 1$ is inversely proportional to the tolerance.

Overall, the computational complexity to solve (P1) is given by $\mathcal{O}(KN)$. Note that the complexity of the proposed solution is linear in the number N of fading blocks, and thus, it is much lower than the exponential complexity $\mathcal{O}(M^N)$ required by the exhaustive searching, where $M \geq 2$, which is related to the searching resolution. Since N is large in practice, the complexity reduction by Theorem 1 is indeed significant.

B. Suboptimal Solution to (P1)

The computational complexity of the optimal solution to (P1) in Theorem 1 is low. Unfortunately, the complexity of the solution in Theorem 1 might not be low enough for certain practical applications, because it is proportional to both N and K . For example, when $K \geq N$, the complexity is higher than $\mathcal{O}(N^2)$. In the practical fading scenario and from the practical implementation perspective, it is very desirable to achieve the complexity proportional only to the number N of the fading blocks, i.e., in the order of $\mathcal{O}(N)$ [30]. However, in (P1), it is very challenging to reduce the complexity while guaranteeing the optimality. To address this issue, in this subsection, we propose a suboptimal solution to (P1) in closed form (up to the Lagrange multiplier λ^{NL}), which turns out to be asymptotically optimal in the low SNR region.

The fundamental idea is to maximize the lower bound of the average rate rather than the actual average rate. To this

$$\rho_{\nu}^{\text{NL}} = \begin{cases} 0, & \text{for Case 1} \\ \rho_{o,\nu}^{\text{NL}}, & \text{if } R_{\nu}(P, \rho_{o,\nu}^{\text{NL}}) + \lambda^{\text{NL}} Q_{\nu}^{\text{NL}}(P, \rho_{o,\nu}^{\text{NL}}) > R_{\nu}(P, 0) \\ 0, & \text{otherwise} \\ 1, & \text{if } \lambda^{\text{NL}} Q_{\nu}^{\text{NL}}(P, 1) > R_{\nu}(P, 0) \\ 0, & \text{otherwise} \\ \rho_{o,\nu}^{\text{NL}}, & \text{for Case 4} \\ 1, & \text{for Case 5} \end{cases} \quad (9)$$

$$\begin{aligned} \gamma(h_{\nu}) \geq \frac{\lambda^{\text{NL}}}{4} & \quad \text{for Case 1} \\ \lambda^{\text{NL}} f(0) \leq g(h_{\nu}), \lambda^{\text{NL}} f(h_{\nu}) < g(0), \text{ and } \gamma(h_{\nu}) < \frac{\lambda^{\text{NL}}}{4} & \quad \text{for Case 2} \\ \lambda^{\text{NL}} f(0) \leq g(h_{\nu}) \text{ and } \lambda^{\text{NL}} f(h_{\nu}) \geq g(0) & \quad \text{for Case 3} \\ \lambda^{\text{NL}} f(0) > g(h_{\nu}), \lambda^{\text{NL}} f(h_{\nu}) < g(0), \text{ and } \gamma(h_{\nu}) < \frac{\lambda^{\text{NL}}}{4} & \quad \text{for Case 4} \\ \lambda^{\text{NL}} f(0) > g(h_{\nu}) \text{ and } \lambda^{\text{NL}} f(h_{\nu}) \geq g(0) & \quad \text{for Case 5.} \end{aligned} \quad (10)$$

$$\rho_{\nu}^{\text{NL}'} = \begin{cases} 0, & \text{for Case 1}' \\ \rho_{so,\nu}^{\text{NL}}, & \text{if } (1 - \rho_{so,\nu}^{\text{NL}}) R_{\nu}(P, 0) + \lambda^{\text{NL}} Q_{\nu}^{\text{NL}}(P, \rho_{so,\nu}^{\text{NL}}) > R_{\nu}(P, 0) \\ 0, & \text{otherwise} \\ 1, & \text{if } \lambda^{\text{NL}} Q_{\nu}^{\text{NL}}(P, 1) > R_{\nu}(P, 0) \\ 0, & \text{otherwise} \\ \rho_{so,\nu}^{\text{NL}}, & \text{for Case 4}' \\ 1, & \text{for Case 5}' \end{cases} \quad (11)$$

end, in the following, we first derive a lower bound of the average rate.

Lemma 2: The objective function of the problem (P1) is lower bounded by

$$\mathbb{E}[R_{\nu}(P, \rho_{\nu})] \geq \mathbb{E}[(1 - \rho_{\nu}) R_{\nu}(P, 0)]. \quad (13)$$

Proof: Since $R_{\nu}(P, \rho_{\nu})$ is concave in $(1 - \rho_{\nu})$ [3], it follows that $R_{\nu}(P, \rho_{\nu}) \geq (1 - \rho_{\nu}) R_{\nu}(P, 0)$, $\forall \nu$ [31]. ■

The lower bound of (13) becomes tight when $\rho_{\nu} \in \{0, 1\}$, $\forall \nu$. Replacing the objective function of (P1) by the lower bound of (13), we can formulate the following problem:

$$(P1'): \max_{0 \leq \rho_{\nu} \leq 1, \forall \nu} \mathbb{E}[(1 - \rho_{\nu}) R_{\nu}(P, 0)] \quad (14a)$$

$$\text{s.t. } \mathbb{E}[Q_{\nu}^{\text{NL}}(P, \rho_{\nu})] \geq Q. \quad (14b)$$

In the following, the solution to (P1') is derived.

Theorem 2: The solution to (P1') is given by (11) (shown at the top of this page), where the Cases 1'-5' are given by

$$\begin{aligned} z(h_{\nu}) \geq \frac{\lambda^{\text{NL}}}{4} & \quad \text{for Case 1}' \\ \max \{\lambda^{\text{NL}} f(h_{\nu}), \lambda^{\text{NL}} f(0)\} < z(h_{\nu}) < \frac{\lambda^{\text{NL}}}{4} & \quad \text{for Case 2}' \\ \lambda^{\text{NL}} f(0) \leq z(h_{\nu}) \leq \lambda^{\text{NL}} f(h_{\nu}) & \quad \text{for Case 3}' \\ \lambda^{\text{NL}} f(h_{\nu}) < z(h_{\nu}) < \lambda^{\text{NL}} f(0) & \quad \text{for Case 4}' \\ z(h_{\nu}) \leq \min \{\lambda^{\text{NL}} f(h_{\nu}), \lambda^{\text{NL}} f(0)\} & \quad \text{for Case 5}' \end{aligned} \quad (15)$$

In (15), $f(x) = \frac{e^{-a(xP-b)}}{(1+e^{-a(xP-b)})^2}$ and $z(x) = \frac{1-\Omega}{P_s Tax P} \log_2 (1 + \frac{xP}{\sigma^2})$. Also, $\rho_{so,\nu}^{\text{NL}}$ is given by

$$\rho_{so,\nu}^{\text{NL}} = \frac{1}{h_{\nu} P} \left(-\frac{1}{a} \ln \left(\frac{2}{1 + \sqrt{1 - \frac{4z(h_{\nu})}{\lambda^{\text{NL}}}}} - 1 \right) + b \right). \quad (16)$$

The constant $\lambda^{\text{NL}} > 0$ is chosen to satisfy $\mathbb{E}[Q_{\nu}^{\text{NL}}(P, \rho_{\nu}^{\text{NL}'})] = Q$.

Proof: The result can be proved by following the similar procedures in Appendix B and replacing the objective function $\mathbb{E}[R_{\nu}(P, \rho_{\nu})]$ by the lower bound $\mathbb{E}[(1 - \rho_{\nu}) R_{\nu}(P, 0)]$, where $\rho_{so,\nu}^{\text{NL}}$ in (16) is given by the solution of the equation $\Psi_{\nu}(P, x) = \frac{1}{2} + \sqrt{\frac{1}{4} - \frac{z(h_{\nu})}{\lambda^{\text{NL}}}}$ over $x \in \left(\frac{b}{h_{\nu} P}, 1\right)$. ■

Note that the solution in Theorem 2 can be computed more efficiently than the optimal solution in Theorem 1. Specifically, only a single positive scalar λ^{NL} needs to be computed numerically. Consequently, the complexity of the solution in Theorem 2 is given by $\mathcal{O}(N)$, which is proportional only to N , and thus, is much lower than the complexity $\mathcal{O}(KN)$ of the optimal solution. But, the solution in Theorem 2 is generally suboptimal to (P1) because the lower bound of (13) is used rather than the exact value. Interestingly and fortunately, we can show that the solution in Theorem 2 is asymptotically optimal in the low SNR regime.

Lemma 3: When $\frac{P}{\sigma^2} \rightarrow 0$, the solution in Theorem 2 is optimal to (P1).

Proof: It follows that $R_\nu(P, \rho_\nu) \rightarrow \frac{(1-\rho_\nu)h_\nu P}{\sigma^2 \ln 2}$ and $(1-\rho_\nu)R_\nu(P, 0) \rightarrow \frac{(1-\rho_\nu)h_\nu P}{\sigma^2 \ln 2}$, as $\frac{P}{\sigma^2} \rightarrow 0$ [15]. Thus, when $\frac{P}{\sigma^2} \rightarrow 0$, the gap between the actual objective value of (P1) and the lower bound of (13) approaches zero, i.e., $R_\nu(P, \rho_\nu) - (1-\rho_\nu)R_\nu(P, 0) \rightarrow 0$, implying that the solution in Theorem 2 is optimal to (P1). ■

Although we can mathematically show the optimality of the solution in Theorem 2 only in the low SNR range, the numerical results in Section V will demonstrate that the performance of this solution is essentially the same as the optimal performance even in the moderate to high SNR range.

C. Comparisons to Existing Schemes

In this subsection, to obtain new and useful insights, we compare the proposed scheme to the existing schemes of [8], [14]. For comparison, in the following, we first present the existing dynamic power splitting scheme for the linear EH [14, Proposition 4.1]:

$$\rho_\nu^L = \begin{cases} \rho_{o,\nu}^L, & \text{if } h_\nu > x_1^L \\ 0, & \text{otherwise} \end{cases} \quad (17)$$

where $\rho_{o,\nu}^L = 1 - \frac{1}{h_\nu P} \left(\frac{1}{\zeta \lambda^L} - \sigma^2 \right)$. Also, $x_1^L = \frac{1}{P} \left(\frac{1}{\zeta \lambda^L} - \sigma^2 \right)$. The constant $0 < \lambda^L \leq \frac{1}{\zeta \sigma^2}$ is determined such that $\mathbb{E}[Q_\nu^L(P, \rho_\nu^L)] = Q$. Next, we present the existing mode switching scheme for the nonlinear EH [8, Lemma 2]:

$$\varrho_\nu^{\text{NL}} = \begin{cases} 1, & \text{if } \chi_1^{\text{NL}} < h_\nu < \chi_2^{\text{NL}} \\ 0, & \text{otherwise} \end{cases} \quad (18)$$

where χ_1^{NL} and $\chi_2^{\text{NL}} (> \chi_1^{\text{NL}})$ are the two roots of the equation $\lambda^{\text{NL}} q^{\text{NL}}(x) = r(x)$, where $q^{\text{NL}}(x) = \frac{P_s T \left(\frac{1}{1+e^{-a(xP-b)}} - \Omega \right)}{1-\Omega}$ and $r(x) = \log_2 \left(1 + \frac{xP}{\sigma^2} \right)$. Also, the constant $\lambda^{\text{NL}} > 0$ is determined such that $\mathbb{E}[Q_\nu^{\text{NL}}(P, \varrho_\nu^{\text{NL}})] = Q$. Note that the existing mode switching result of (18) can be considered as a special case of our result in Theorem 1 (or Theorem 2) for the Case 3 (or Case 3').

In Fig. 1, we illustrate the proposed and existing schemes. In this figure, for notational simplicity, we focus on a particular fading state, and thus, we drop the index ν from the relevant expressions. Also, in Fig. 1, the term "PS" means the power splitting, i.e., both ID and EH. In Fig. 1(c), x_1^{NL} , $(x_2^{\text{NL}}, x_4^{\text{NL}})$, and x_3^{NL} denote the roots of the equations $\gamma(x) = \frac{1}{4}$, $\lambda_{\text{NL}} f(x) = g(0)$, and $\lambda_{\text{NL}} f(0) = g(x)$, respectively. For the illustration purpose, we assume that $x_j^{\text{NL}} < x_{j+1}^{\text{NL}}$, $j = 1, 2, 3$. Comparing the proposed and existing schemes, we can obtain the following insights:

- From Figs. 1(a) and 1(c), and the results of (9) and (17), one can see that the optimal dynamic power splitting schemes for the linear EH and the nonlinear EH are fundamentally different: For example, for the case of linear EH, the received power is used for the two different purposes: only for ID with $\rho^L = 0$ or for both ID and EH with $0 < \rho^L < 1$. Thus, in the linear EH, there are *two* different regions for the optimal dynamic power splitting. On the other hand, for the case of nonlinear EH, the

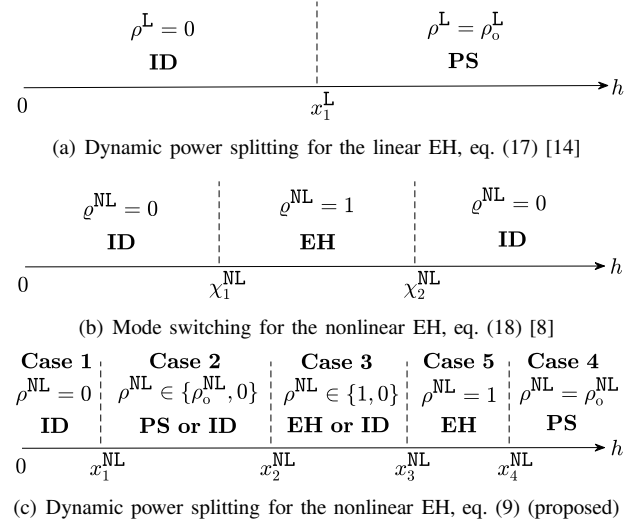


Fig. 1. Comparison of the proposed and existing schemes for the case of CSIR.

received power is used for the three different purposes: only for ID with $\rho^{\text{NL}} = 0$, only for EH with $\rho^{\text{NL}} = 1$, or for both ID and EH with $0 < \rho^{\text{NL}} < 1$. Consequently, in the nonlinear EH, there are up to *five* different regions for the optimal dynamic power splitting. Also, for the case of linear EH, the optimal power splitting ratio increases as the channel gain increases, and thus, the power used for EH increases. On the other hand, for the case of nonlinear EH, the optimal power splitting ratio (and also, the power used for EH) increases, and then, decreases as the channel gain increases.

- From Figs. 1(b) and 1(c), and the results of (9) and (18), one can see that for the case of nonlinear EH, the optimal dynamic power splitting scheme is very different from the optimal mode switching scheme: For example, in the mode switching, the optimal power splitting ratio ϱ_ν^{NL} takes two *binary* values between 0 and 1, i.e., $\varrho_\nu^{\text{NL}} \in \{0, 1\}$. Thus, the received power is used for the two different purposes: only for EH or only for ID. Consequently, in the mode switching, there are *three* different regions for the optimal power splitting. On the other hand, in the dynamic power splitting, the optimal power splitting ratio ρ_ν^{NL} is *continuous* between 0 and 1, i.e., $\rho_\nu^{\text{NL}} \in [0, 1]$. Also, the received power is used for the three different purposes: only for ID, only for EH, or for both ID and EH. Consequently, in the dynamic power splitting, there are up to *five* different regions for the optimal power splitting.

IV. DYNAMIC POWER SPLITTING FOR NONLINEAR EH WITH CSIT

In this section, we consider the case of CSIT. We first derive the optimal solution to (P2). Then a suboptimal solution to (P2) is proposed with low complexity. Finally, we compare the proposed and existing schemes.

A. Optimal Solution to (P2)

In order to solve (P2), in the following, we first define the time-sharing condition for (P2).

Definition 2 ([30, Definition 1]): Let $\{P_{x,\nu}, \rho_{x,\nu}\}$ and $\{P_{y,\nu}, \rho_{y,\nu}\}$ denote the optimal solutions to the problem (P2) when $(Q, P_{\text{avg}}) = (Q_x, \bar{P}_x)$ and $(Q, P_{\text{avg}}) = (Q_y, \bar{P}_y)$, respectively. It is said that (P2) satisfies the *time-sharing* condition (or time-sharing property) if there exists a feasible solution $\{P_{z,\nu}, \rho_{z,\nu}\}$ such that $\mathbb{E}[Q_{\nu}^{\text{NL}}(P_{z,\nu}, \rho_{z,\nu})] \geq \theta Q_x + (1 - \theta)Q_y$, $\mathbb{E}[P_{z,\nu}] \leq \theta \bar{P}_x + (1 - \theta) \bar{P}_y$, and $\mathbb{E}[R_{\nu}(P_{z,\nu}, \rho_{z,\nu})] \geq \theta \mathbb{E}[R_{\nu}(P_{x,\nu}, \rho_{x,\nu})] + (1 - \theta) \mathbb{E}[R_{\nu}(P_{y,\nu}, \rho_{y,\nu})]$ for any $0 \leq \theta \leq 1$. \blacksquare

Now, we establish the time-sharing property of (P2).

Lemma 4: In the problem (P2), the time-sharing condition is satisfied.

Proof: See Appendix A. \blacksquare

From Lemma 4, the optimal solution to (P2) can be obtained by using the Lagrange duality method, similar to (P1). However, even when the Lagrange duality method is used, the problem (P2) is still very difficult to solve (much more difficult than (P1)), because the variables $\{\rho_{\nu}\}$ and $\{P_{\nu}\}$ are coupled. To overcome the difficulty, we take the following approach: we first convert the problem (P2) into a more tractable form, and then, we derive the solution by solving the converted problem. Taking this approach, we have the following result.

Theorem 3: The solution to (P2) is given by

$$P_{\nu}^{\text{NL}} = P_{\text{ID},\nu}^{\text{NL}} + P_{\text{EH},\nu}^{\text{NL}}, \quad (24a)$$

$$\rho_{\nu}^{\text{NL}} = \begin{cases} 0, & \text{if } P_{\text{ID},\nu}^{\text{NL}} = P_{\text{EH},\nu}^{\text{NL}} = 0 \\ \frac{P_{\text{EH},\nu}^{\text{NL}}}{P_{\text{ID},\nu}^{\text{NL}} + P_{\text{EH},\nu}^{\text{NL}}}, & \text{otherwise} \end{cases}. \quad (24b)$$

In (24), $P_{\text{ID},\nu}^{\text{NL}}$ is given by

$$P_{\text{ID},\nu}^{\text{NL}} = \begin{cases} 0, & \text{if } h_{\nu} \leq \mu^{\text{NL}} \sigma^2 \\ \min \left\{ \frac{1}{\mu^{\text{NL}}} - \frac{\sigma^2}{h_{\nu}}, P_{\text{max}} - P_{\text{EH},\nu}^{\text{NL}} \right\}, & \text{if } h_{\nu} > \mu^{\text{NL}} \sigma^2 \end{cases}. \quad (25)$$

Also, $P_{\text{EH},\nu}^{\text{NL}}$ is given by (19) (shown at the top of the next page), where $P_{\text{th},\nu} = \max \left\{ P_{\text{max}} - \frac{1}{\mu^{\text{NL}}} + \frac{\sigma^2}{h_{\nu}}, 0 \right\}$. In (19), $[P_{\text{EH},\nu}^{\text{NL}}]_{P_{\text{low}}^{\text{up}}}^{P_{\text{up}}}$ is given by (20) (shown at the top of the next page), where the Cases A.1–A.5 are given by (21) (shown at the top of the next page). Also, $[P_{\text{EH},\nu}^{\text{NL}}]_{P_{\text{low}}^{\text{up}}}^{P_{\text{up}}}$ is given by (22) (shown at the top of the next page), where the Cases B.1–B.5 are given by (23) (shown at the top of the next page). In (21) and (23), $F_{\text{low}/\text{up}}(x) = \frac{e^{-a(xP_{\text{low}/\text{up}} - b)}}{(1 + e^{-a(xP_{\text{low}/\text{up}} - b)})^2}$,

$G_{\text{low}/\text{up}}(x) = \frac{1 - \Omega}{P_s Ta(x(P_{\text{max}} - P_{\text{low}/\text{up}}) + \sigma^2)}$, $Z(x) = \frac{1 - \Omega}{P_s Ta x}$, and $\Gamma(x) = \frac{1 - \Omega}{P_s Ta(\max\{xP_{\text{max}} - b, 0\} + \sigma^2)}$. In (20), $P_{\text{o},\nu}^A$ is given by

$$P_{\text{o},\nu}^A = \frac{1}{h_{\nu}} \left(-\frac{1}{a} \ln \left(\frac{2}{1 + \sqrt{1 - \frac{4\mu^{\text{NL}}Z(h_{\nu})}{\lambda^{\text{NL}}}}} - 1 \right) + b \right). \quad (26)$$

In (22), $P_{\text{o},\nu}^B$ is the root of the following equation:

$$\lambda^{\text{NL}} \Psi_{\nu}(x, 1) (1 - \Psi_{\nu}(x, 1)) = \frac{1 - \Omega}{P_s Ta (h_{\nu}(P_{\text{max}} - x) + \sigma^2)} \quad (27)$$

over $x \in \left(\frac{b}{h_{\nu}}, P_{\text{up}} \right)$. The constants $\lambda^{\text{NL}} > 0$ and $\mu^{\text{NL}} > 0$ are chosen to satisfy $\mathbb{E}[Q_{\nu}^{\text{NL}}(P_{\nu}^{\text{NL}}, \rho_{\nu}^{\text{NL}})] = Q$ and $\mathbb{E}[P_{\nu}^{\text{NL}}] = P_{\text{avg}}$.

Proof: See Appendix C. \blacksquare

The result of Theorem 3 can be intuitively interpreted as follows. First, at each fading state, the values of $P_{\text{ID},\nu}^{\text{NL}}$ and $P_{\text{EH},\nu}^{\text{NL}}$ are determined according to (25) and (19), respectively, which can be considered as the optimal power allocation for ID and EH. Then the optimal transmit power is set to the total amount of power assigned to both ID and EH, i.e., $P_{\nu}^{\text{NL}} = P_{\text{ID},\nu}^{\text{NL}} + P_{\text{EH},\nu}^{\text{NL}}$. Also, the optimal power splitting ratio is set to the fraction of power assigned to EH, i.e., $\rho_{\nu}^{\text{NL}} = \frac{P_{\text{EH},\nu}^{\text{NL}}}{P_{\text{ID},\nu}^{\text{NL}} + P_{\text{EH},\nu}^{\text{NL}}}$, and it is set to zero if the optimal transmit power is zero.

From Theorem 3, the optimal solution to (P2) can be computed very efficiently. In the proposed solution, the positive scalars λ^{NL} , μ^{NL} , and $\{P_{\nu}^B\}$ need to be computed numerically. The values of λ^{NL} and μ^{NL} can be found efficiently via the sub-gradient method as follows [30]: $\lambda^{i+1} = \max \left\{ \lambda^i - s^i (\mathbb{E}[Q_{\nu}^{\text{NL}}(P_{\text{avg}}, \rho_{\nu}^{\text{NL}})] - Q), 0 \right\}$ and $\mu^{i+1} = \max \left\{ \mu^i - s^i (P_{\text{avg}} - \mathbb{E}[P_{\nu}^{\text{NL}}]), 0 \right\}$, where i denotes the iteration number, λ^i and μ^i the values of λ^{NL} and μ^{NL} , respectively, at the i th iteration, and $s^i > 0$ the step size at the i th iteration. Also, the value of P_{ν}^B can be found efficiently by solving the nonlinear equation of (30) using the one-dimensional searching, e.g., the bisection method [31]. Overall, the computational complexity to solve (P2) is given by $\mathcal{O}(KN)$, where $K > 1$. This complexity is linear in the number N of the fading blocks, and thus, it is much lower than the exponential complexity $\mathcal{O}(M^N)$ of the exhaustive searching, where $M \geq 2$.

So far, we have studied the problem (P2) under both the long-term and short-term power constraints. Now, relaxing the short-term power constraint, we further investigate the problem (P2) only with the long-term power constraint to obtain the theoretically largest R-E region of the dynamic power splitting scheme. Note that for the case of CSIT, the theoretically best performance of the SWIPT system in the fading channel can be achieved when only the long-term power constraint is imposed [9]. Interestingly, in the following, we show that only with the long-term power constraint, it is possible to even further reduce the computational complexity to solve (P2) (while achieving the theoretically best performance).

Lemma 5: The solution to (P2) only with the long-term power constraint is given by (24) with $P_{\text{ID},\nu}^{\text{NL}}$ and $P_{\text{EH},\nu}^{\text{NL}}$ replaced by $P_{\text{ID},\nu}^{\text{NL}'}$ and $P_{\text{EH},\nu}^{\text{NL}'}$, respectively, where

$$P_{\text{ID},\nu}^{\text{NL}'} = \max \left\{ \frac{1}{\mu^{\text{NL}}} - \frac{\sigma^2}{h_{\nu}}, 0 \right\}, \quad (28a)$$

$$P_{\text{EH},\nu}^{\text{NL}'} = \begin{cases} 0, & \text{for Case A.1}' \\ \begin{cases} P_{\text{o},\nu}^A, & \text{if } \lambda^{\text{NL}} Q_{\nu}^{\text{NL}}(P_{\text{o},\nu}^A, 1) \\ & > \mu^{\text{NL}} P_{\text{o},\nu}^A \\ 0, & \text{otherwise} \end{cases}, & \text{for Case A.2}' \\ P_{\text{o},\nu}^A, & \text{for Case A.3}' \end{cases}. \quad (28b)$$

In (28b), $P_{\text{o},\nu}^A$ is given by (26). Also, the Cases A.1'–A.3' are

$$P_{\text{EH},\nu}^{\text{NL}} = \begin{cases} \left[P_{\text{EH},\nu}^A \right]_0^{P_{\text{max}}}, & \text{if } h_\nu \leq \mu^{\text{NL}} \sigma^2 \\ \left[P_{\text{EH},\nu}^A \right]_0^{P_{\text{th},\nu}}, & \text{if } \log_2 \left(\frac{h_\nu}{\lambda^{\text{NL}} \sigma^2} \right) + \frac{\lambda^{\text{NL}} \sigma^2}{h_\nu} - 1 + \lambda^{\text{NL}} Q_\nu^{\text{NL}} \left(\left[P_{\text{EH},\nu}^A \right]_0^{P_{\text{th},\nu}}, 1 \right) - \mu^{\text{NL}} \cdot \left[P_{\text{EH},\nu}^A \right]_0^{P_{\text{th},\nu}} \\ > R_\nu \left(P_{\text{max}} - \left[P_{\text{EH},\nu}^B \right]_0^{P_{\text{max}}}, 0 \right) + \lambda^{\text{NL}} Q_\nu^{\text{NL}} \left(\left[P_{\text{EH},\nu}^B \right]_0^{P_{\text{max}}}, 1 \right) - \mu^{\text{NL}} P_{\text{max}}, & \text{if } h_\nu > \mu^{\text{NL}} \sigma^2 \\ \left[P_{\text{EH},\nu}^B \right]_0^{P_{\text{th},\nu}}, & \text{otherwise} \end{cases} \quad (19)$$

$$\left[P_{\text{EH},\nu}^A \right]_0^{P_{\text{up}}} = \begin{cases} P_{\text{low}}, & \text{for Case A.1} \\ \left\{ \begin{array}{l} P_{\text{o},\nu}^A, \text{ if } \lambda^{\text{NL}} Q_\nu^{\text{NL}}(P_{\text{o},\nu}^A, 1) - \mu^{\text{NL}} P_{\text{o},\nu}^A > \lambda^{\text{NL}} Q_\nu^{\text{NL}}(P_{\text{low}}, 1) - \mu^{\text{NL}} P_{\text{low}}, \\ P_{\text{low}}, \text{ otherwise} \end{array} \right. & \text{for Case A.2} \\ \left\{ \begin{array}{l} P_{\text{up}}, \text{ if } \lambda^{\text{NL}} Q_\nu^{\text{NL}}(P_{\text{up}}, 1) - \mu^{\text{NL}} P_{\text{up}} > \lambda^{\text{NL}} Q_\nu^{\text{NL}}(P_{\text{low}}, 1) - \mu^{\text{NL}} P_{\text{low}}, \\ P_{\text{low}}, \text{ otherwise} \end{array} \right. & \text{for Case A.3} \\ P_{\text{o},\nu}^A, & \text{for Case A.4} \\ P_{\text{up}}, & \text{for Case A.5} \end{cases} \quad (20)$$

$$\begin{aligned} \mu^{\text{NL}} Z(h_\nu) \geq \frac{\lambda^{\text{NL}}}{4} & \quad \text{for Case A.1} \\ \max \{ \lambda^{\text{NL}} F_{\text{up}}(h_\nu), \lambda^{\text{NL}} F_{\text{low}}(h_\nu) \} < \mu^{\text{NL}} Z(h_\nu) < \frac{\lambda^{\text{NL}}}{4} & \quad \text{for Case A.2} \\ \lambda^{\text{NL}} F_{\text{low}}(h_\nu) \leq \mu^{\text{NL}} Z(h_\nu) \leq \lambda^{\text{NL}} F_{\text{up}}(h_\nu) & \quad \text{for Case A.3} \\ \lambda^{\text{NL}} F_{\text{up}}(h_\nu) \leq \mu^{\text{NL}} Z(h_\nu) \leq \lambda^{\text{NL}} F_{\text{low}}(h_\nu) & \quad \text{for Case A.4} \\ \mu^{\text{NL}} Z(h_\nu) \leq \min \{ \lambda^{\text{NL}} F_{\text{up}}(h_\nu), \lambda^{\text{NL}} F_{\text{low}}(h_\nu) \} & \quad \text{for Case A.5.} \end{aligned} \quad (21)$$

$$\left[P_{\text{EH},\nu}^B \right]_0^{P_{\text{up}}} = \begin{cases} P_{\text{low}}, & \text{for Case B.1} \\ \left\{ \begin{array}{l} P_{\text{o},\nu}^B, \text{ if } R_\nu(P_{\text{up}} - P_{\text{o},\nu}^B, 0) + \lambda^{\text{NL}} Q_\nu^{\text{NL}}(P_{\text{o},\nu}^B, 1) > R_\nu(P_{\text{up}} - P_{\text{low}}, 0) + \lambda^{\text{NL}} Q_\nu^{\text{NL}}(P_{\text{low}}, 1), \\ P_{\text{low}}, \text{ otherwise} \end{array} \right. & \text{for Case B.2} \\ \left\{ \begin{array}{l} P_{\text{up}}, \text{ if } \lambda^{\text{NL}} Q_\nu^{\text{NL}}(P_{\text{up}}, 1) > R_\nu(P_{\text{up}} - P_{\text{low}}, 0) + \lambda^{\text{NL}} Q_\nu^{\text{NL}}(P_{\text{low}}, 1), \\ P_{\text{low}}, \text{ otherwise} \end{array} \right. & \text{for Case B.3} \\ P_{\text{o},\nu}^B, & \text{for Case B.4} \\ P_{\text{up}}, & \text{for Case B.5} \end{cases} \quad (22)$$

$$\begin{aligned} \Gamma(h_\nu) \geq \frac{\lambda^{\text{NL}}}{4} & \quad \text{for Case B.1} \\ \lambda^{\text{NL}} F_{\text{low}}(h_\nu) \leq G_{\text{low}}(h_\nu), \lambda^{\text{NL}} F_{\text{up}}(h_\nu) < G_{\text{up}}(h_\nu), \text{ and } \Gamma(h_\nu) < \frac{\lambda^{\text{NL}}}{4} & \quad \text{for Case B.2} \\ \lambda^{\text{NL}} F_{\text{low}}(h_\nu) \leq G_{\text{low}}(h_\nu), \lambda^{\text{NL}} F_{\text{up}}(h_\nu) \geq G_{\text{up}}(h_\nu), \text{ and } \Gamma(h_\nu) < \frac{\lambda^{\text{NL}}}{4} & \quad \text{for Case B.3} \\ \lambda^{\text{NL}} F_{\text{low}}(h_\nu) > G_{\text{low}}(h_\nu), \lambda^{\text{NL}} F_{\text{up}}(h_\nu) < G_{\text{up}}(h_\nu), \text{ and } \Gamma(h_\nu) < \frac{\lambda^{\text{NL}}}{4} & \quad \text{for Case B.4} \\ \lambda^{\text{NL}} F_{\text{low}}(h_\nu) > G_{\text{low}}(h_\nu), \lambda^{\text{NL}} F_{\text{up}}(h_\nu) \geq G_{\text{up}}(h_\nu), \text{ and } \Gamma(h_\nu) < \frac{\lambda^{\text{NL}}}{4} & \quad \text{for Case B.5.} \end{aligned} \quad (23)$$

given by

$$\begin{aligned} h_\nu & \leq x_{\text{EH},1}^{\text{NL}'} & \text{for Case A.1}' \\ x_{\text{EH},1}^{\text{NL}'} & < h_\nu < x_{\text{EH},2}^{\text{NL}'} & \text{for Case A.2}' \\ h_\nu & \geq x_{\text{EH},2}^{\text{NL}'} & \text{for Case A.3}' \end{aligned} \quad (29)$$

where $x_{\text{EH},1}^{\text{NL}'} = \frac{4\mu^{\text{NL}}(1-\Omega)}{\lambda^{\text{NL}} P_s T_a}$ and $x_{\text{EH},2}^{\text{NL}'} = \frac{\mu^{\text{NL}}}{\lambda^{\text{NL}} \Omega P_s T_a} (> x_{\text{EH},1}^{\text{NL}'})$ are the roots of the equations $\mu^{\text{NL}} Z(x) = \frac{\lambda^{\text{NL}}}{4}$ and $\mu^{\text{NL}} Z(x) = \lambda^{\text{NL}} F_{\text{low}}(x)$ with $P_{\text{low}} = 0$, respectively. The constants $\lambda^{\text{NL}} > 0$ and $\mu^{\text{NL}} > 0$ are determined such that $\mathbb{E}[Q_\nu^{\text{NL}}(P_\nu^{\text{NL}}, \rho_\nu^{\text{NL}})] =$

Q and $\mathbb{E}[P_\nu^{\text{NL}}] = P_{\text{avg}}$.

Proof: To relax the short-term power constraint, we take $P_{\text{max}} \rightarrow \infty$. From (25), it follows that $P_{\text{ID},\nu}^{\text{NL}} \rightarrow \max \left\{ \frac{1}{\mu^{\text{NL}}} - \frac{\sigma^2}{h_\nu}, 0 \right\}$ as $P_{\text{max}} \rightarrow \infty$. Also, from (19), we have $P_{\text{EH},\nu}^{\text{NL}} \rightarrow \left[P_{\text{EH},\nu}^A \right]_0^\infty$ as $P_{\text{max}} \rightarrow \infty$. Since $F_{\text{up}}(h_\nu) \rightarrow 0$ as $P_{\text{up}} \rightarrow \infty$, the Cases A.3 and A.5 disappear from (21). Also, the Cases A.1, A.2, and A.4 become the Cases A.1', A.2', and A.3', respectively. Thus, the result of (28) follows. ■

From Lemma 5, only with the long-term power constraint, the optimal solution to (P2) can be computed extremely

efficiently. Specifically, only the two positive scalars λ^{NL} and μ^{NL} need to be determined numerically. Consequently, the complexity is given by $\mathcal{O}(N)$, which is proportional only to N .

B. Suboptimal Solution to (P2)

The computational complexity of the optimal solution to (P2) in Theorem 3 is low; but, the complexity is proportional to both N and K . Thus, the complexity might not be low enough for certain practical applications. On the other hand, the complexity of the solution in Lemma 5 is always low enough since its complexity is proportional only to N . However, this solution can be used only when the short-term power constraint is relaxed (i.e., only the long-term power constraint is imposed). In the practical system, considering the short-term power constraint is often meaningful because the short-term power is usually limited by the regulation bodies such as the FCC [32]. Therefore, in general, one needs to use the solution in Theorem 3. In this subsection, to overcome the above limitations, we present a suboptimal solution to (P2) in closed form without relaxing the short-term power constraint. This solution turns out to be asymptotically optimal in the low SNR regime.

In order to derive a suboptimal solution, we define $P_{\text{EH},\nu} = \rho_\nu P_\nu$, $\forall \nu$, each of which denotes the power allocation for EH at each fading state. Using the result of Theorem 3, it can be shown that when $h_\nu \leq \mu^{\text{NL}} \sigma^2$ and $P_{\text{th},\nu} \leq P_{\text{EH},\nu} \leq P_{\text{max}}$, the optimization of (P2) reduces to the following optimization (the detailed proof is given in Appendix C):

$$\max_{P_{\text{th},\nu} < P_{\text{EH},\nu} \leq P_{\text{max}}} R_\nu(P_{\text{max}} - P_{\text{EH},\nu}, 0) + \lambda^{\text{NL}} Q_\nu^{\text{NL}}(P_{\text{EH},\nu}, 1). \quad (30)$$

To carry out the above optimization, the value of $P_{\text{o},\nu}^B$ needs to be computed numerically by solving the nonlinear equation of (30), which in turn increases the complexity. To address the complexity issue and to obtain a closed form solution, we take the following approach: we use the lower bound of the objective function of (30) for the optimization instead of the actual objective function. To this end, in the following, we derive the lower bound of the objective function of (30).

Lemma 6: The objective function of (30) is lower bounded by

$$R_\nu(P_{\text{max}} - P_{\text{EH},\nu}, 0) + \lambda^{\text{NL}} Q_\nu^{\text{NL}}(P_{\text{EH},\nu}, 1) \geq \left(1 - \frac{P_{\text{EH},\nu}}{P_{\text{max}}}\right) R_\nu(P_{\text{max}}, 0) + \lambda^{\text{NL}} Q_\nu^{\text{NL}}(P_{\text{EH},\nu}, 1). \quad (31)$$

Proof: Since $R_\nu(P_{\text{max}} - P_{\text{EH},\nu}, 0) = \log_2 \left(1 + \frac{h_\nu(P_{\text{max}} - P_{\text{EH},\nu})}{\sigma^2}\right)$ is concave in $\left(1 - \frac{P_{\text{EH},\nu}}{P_{\text{max}}}\right)$, it follows that $R_\nu(P_{\text{max}} - P_{\text{EH},\nu}, 0) \geq \left(1 - \frac{P_{\text{EH},\nu}}{P_{\text{max}}}\right) R_\nu(P_{\text{max}}, 0)$ [31]. ■

The lower bound of (31) in Lemma 6 becomes tight when $P_{\text{EH},\nu} = P_{\text{max}}$. Replacing the objective function of (30) with

the lower bound of (31), we have the following optimization problem:

$$(\text{P2}'): \max_{P_{\text{th},\nu} < P_{\text{EH},\nu} \leq P_{\text{max}}} \left\{ \left(1 - \frac{P_{\text{EH},\nu}}{P_{\text{max}}}\right) R_\nu(P_{\text{max}}, 0) + \lambda^{\text{NL}} Q_\nu^{\text{NL}}(P_{\text{EH},\nu}, 1) \right\}. \quad (32)$$

In the following, the solution to (P2') is derived.

Theorem 4: The solution to (P2') is given by $[P_{\text{EH},\nu}^B]_{P_{\text{th},\nu}}^{P_{\text{max}}}$, where $[P_{\text{EH},\nu}^B]_{P_{\text{th},\nu}}^{P_{\text{up}}}$ is given by (33) (shown at the top of the next page). In (33), the Cases B.1'–B.5' are given by (34) (shown at the top of the next page), where $Z'(x) = \frac{1-\Omega}{s_T \alpha x P_{\text{max}}} \log_2 \left(1 + \frac{x P_{\text{max}}}{\sigma^2}\right)$. Also, $P_{\text{so},\nu}^B$ is given by

$$P_{\text{so},\nu}^B = \frac{1}{h_\nu} \left(-\frac{1}{a} \ln \left(\frac{2}{1 + \sqrt{1 - \frac{4Z'(h_\nu)}{\lambda^{\text{NL}}}}} - 1 \right) + b \right). \quad (35)$$

Proof: The result can be proved by following the similar procedures in Appendix C, where $P_{\text{so},\nu}^B$ in (35) is given by the solution of the equation $\Psi_\nu(x, 1) = \frac{1}{2} + \sqrt{\frac{1}{4} - \frac{Z'(h_\nu)}{\lambda^{\text{NL}}}}$ over $x \in \left(\frac{b}{h_\nu}, P_{\text{up}}\right)$. ■

Using Theorem 4, the suboptimal solution to (P2) can be obtained from the result of Theorem 3 with $[P_{\text{EH},\nu}^B]_{P_{\text{th},\nu}}^{P_{\text{max}}}$ replaced by $[P_{\text{EH},\nu}^B]_{P_{\text{th},\nu}}^{P_{\text{max}}}$. Note that the computational complexity of this solution is extremely low: only the two positive scalars λ^{NL} and μ^{NL} need to be computed numerically. Thus, the complexity is given by $\mathcal{O}(N)$, which is proportional only to N and is even lower than the complexity of the optimal solution in Theorem 3. However, the performance of the solution using Theorem 4 is generally suboptimal since the lower bound of (31) is used rather than the exact value. Fortunately and interestingly, we can establish its asymptotic optimality in the low SNR regime, which is presented in the following.

Lemma 7: When $\frac{P_{\text{max}}}{\sigma^2} \rightarrow 0$, the solution in Theorem 3 with $[P_{\text{EH},\nu}^B]_{P_{\text{th},\nu}}^{P_{\text{max}}}$ replaced by $[P_{\text{EH},\nu}^B]_{P_{\text{th},\nu}}^{P_{\text{max}}}$ is optimal to (P2).

Proof: For the proof, it is sufficient to show that the gap between the actual objective value of (30) and the lower bound of (31) goes to zero as $\frac{P_{\text{max}}}{\sigma^2} \rightarrow 0$. When $\frac{P_{\text{max}}}{\sigma^2} \rightarrow 0$, it follows that $R_\nu(P_{\text{max}} - P_{\text{EH},\nu}, 0) \rightarrow \frac{h_\nu(P_{\text{max}} - P_{\text{EH},\nu})}{\sigma^2 \ln 2}$ and $\left(1 - \frac{P_{\text{EH},\nu}}{P_{\text{max}}}\right) R_\nu(P_{\text{max}}, 0) \rightarrow \frac{h_\nu(P_{\text{max}} - P_{\text{EH},\nu})}{\sigma^2 \ln 2}$ [15]. Thus, $R_\nu(P_{\text{max}} - P_{\text{EH},\nu}, 0) - \left(1 - \frac{P_{\text{EH},\nu}}{P_{\text{max}}}\right) R_\nu(P_{\text{max}}, 0) \rightarrow 0$ as $\frac{P_{\text{max}}}{\sigma^2} \rightarrow 0$. ■

Although we can mathematically show the optimality of the solution in Theorem 4 only in the low SNR region, the numerical results in the next section will demonstrate that the performance of this solution is very close to the optimal performance even in the moderate to high SNR range.

C. Comparisons to Existing Schemes

In this subsection, to obtain further insights, the proposed scheme is compared to the existing schemes of [9], [14]. For

$$\begin{aligned}
& [P_{\text{EH},\nu}^{B'}]_{P_{\text{low}}}^{P_{\text{up}}} \\
&= \begin{cases} P_{\text{low}}, & \text{for Case B.1}' \\ \begin{cases} P_{\text{so},\nu}^B, & \text{if } R_\nu(P_{\text{up}} - P_{\text{so},\nu}^B, 0) + \lambda^{\text{NL}} Q_\nu^{\text{NL}}(P_{\text{so},\nu}^B, 1) > R_\nu(P_{\text{up}} - P_{\text{low}}, 0) + \lambda^{\text{NL}} Q_\nu^{\text{NL}}(P_{\text{low}}, 1) \\ P_{\text{low}}, & \text{otherwise} \end{cases}, & \text{for Case B.2}' \\ \begin{cases} P_{\text{up}}, & \text{if } \lambda^{\text{NL}} Q_\nu^{\text{NL}}(P_{\text{up}}, 1) > R_\nu(P_{\text{up}} - P_{\text{low}}, 0) + \lambda^{\text{NL}} Q_\nu^{\text{NL}}(P_{\text{low}}, 1) \\ P_{\text{low}}, & \text{otherwise} \end{cases}, & \text{for Case B.3}' \\ P_{\text{so},\nu}^B, & \text{for Case B.4}' \\ P_{\text{up}}, & \text{for Case B.5}' \end{cases} \quad (33)
\end{aligned}$$

$$\begin{aligned}
& Z'(h_\nu) \geq \frac{\lambda^{\text{NL}}}{4} & \text{for Case B.1}' \\
& \max \{ \lambda^{\text{NL}} F(h_\nu, P_{\text{up}}), \lambda^{\text{NL}} F(h_\nu, P_{\text{low}}) \} < Z'(h_\nu) < \frac{\lambda^{\text{NL}}}{4} & \text{for Case B.2}' \\
& \lambda^{\text{NL}} F(h_\nu, P_{\text{low}}) \leq Z'(h_\nu) \leq \lambda^{\text{NL}} F(h_\nu, P_{\text{up}}) & \text{for Case B.3}' \\
& \lambda^{\text{NL}} F(h_\nu, P_{\text{up}}) \leq Z'(h_\nu) \leq \lambda^{\text{NL}} F(h_\nu, P_{\text{low}}) & \text{for Case B.4}' \\
& Z'(h_\nu) \leq \min \{ \lambda^{\text{NL}} F(h_\nu, P_{\text{up}}), \lambda^{\text{NL}} F(h_\nu, P_{\text{low}}) \} & \text{for Case B.5}' \quad (34)
\end{aligned}$$

comparison, in the following, we first present the existing dynamic power splitting scheme for the linear EH [12, Proposition 4.2]:

$$(P_\nu^L, \rho_\nu^L) = \begin{cases} \begin{cases} (P_{\text{max}}, \rho_{\text{o},\nu}^L), & \text{if } h_\nu > x_1^L \\ \left([P_{\text{o},\nu}^L]_0^{P_{\text{max}}}, 0 \right), & \text{otherwise} \end{cases}, & \text{if } x_2^L \leq x_1^L \\ \begin{cases} (P_{\text{max}}, \rho_{\text{o},\nu}^L), & \text{if } h_\nu > x_2^L \\ \left([P_{\text{o},\nu}^L]_0^\infty, 0 \right), & \text{otherwise} \end{cases}, & \text{if } x_2^L < x_1^L \end{cases} \quad (36)$$

where $[P_{\text{o},\nu}^L]_{P_{\text{low}}}^{P_{\text{up}}} = \min \left\{ \max \left\{ \frac{1}{\mu^L} - \frac{\sigma^2}{h_\nu}, P_{\text{low}} \right\}, P_{\text{up}} \right\}$ and $\rho_{\text{o},\nu}^L = 1 - \frac{1}{h_\nu P_{\text{max}}} \left(\frac{1}{\zeta \lambda^L} - \sigma^2 \right)$. Also, $x_1^L = \frac{1}{P_{\text{max}}} \left(\frac{1}{\zeta \lambda^L} - \sigma^2 \right)$ and $x_2^L = \frac{\mu^L}{\zeta \lambda^L}$. The constants $0 < \lambda^L \leq \frac{1}{\zeta \sigma^2}$ and $\mu^L > 0$ are determined such that $\mathbb{E}[Q_\nu^L(P_\nu^L, \rho_\nu^L)] = Q$ and $\mathbb{E}[P_\nu^L] = P_{\text{avg}}$.

Second, we present the existing mode switching scheme for the nonlinear EH [9, Theorem 2]:

$$(p_\nu^{\text{NL}}, \varrho_\nu^{\text{NL}}) = \begin{cases} (p_{\text{ID},\nu}^{\text{NL}}, 0), & \text{if } R_\nu(p_{\text{ID},\nu}^{\text{NL}}, 0) - \mu^{\text{NL}} p_{\text{ID},\nu}^{\text{NL}} \\ & > \lambda^{\text{NL}} Q_\nu^{\text{NL}}(p_{\text{EH},\nu}^{\text{NL}}, 1) - \mu^{\text{NL}} p_{\text{EH},\nu}^{\text{NL}} \\ (p_{\text{EH},\nu}^{\text{NL}}, 1), & \text{otherwise} \end{cases} \quad (37)$$

where $p_{\text{ID},\nu}^{\text{NL}} = \min \left\{ \max \left\{ \frac{1}{\mu^{\text{NL}}} - \frac{\sigma^2}{h_\nu}, 0 \right\}, P_{\text{max}} \right\}$ and $p_{\text{EH},\nu}^{\text{NL}} = [P_{\text{EH},\nu}^{\text{NL}}]_0^{P_{\text{max}}}$. Also, $[P_\nu^A]_{P_{\text{low}}}^{P_{\text{up}}}$ is given by (20). Only with the long-term power constraint, the mode switching scheme for the nonlinear EH was shown as [9, Lemma 5]

$$(p_\nu^{\text{NL}}, \varrho_\nu^{\text{NL}}) = \begin{cases} (P_{\text{ID},\nu}^{\text{NL}'}, 0), & \text{if } R_\nu(P_{\text{ID},\nu}^{\text{NL}'}, 0) - \mu^{\text{NL}} P_{\text{ID},\nu}^{\text{NL}'} \\ & > \lambda^{\text{NL}} Q_\nu^{\text{NL}}(P_{\text{EH},\nu}^{\text{NL}'}, 1) - \mu^{\text{NL}} P_{\text{EH},\nu}^{\text{NL}'} \\ (P_{\text{EH},\nu}^{\text{NL}'}, 1), & \text{otherwise} \end{cases} \quad (38)$$

where $P_{\text{ID},\nu}^{\text{NL}'}$ and $P_{\text{EH},\nu}^{\text{NL}'}$ are given by (28a) and (28b), respectively. In (37) and (38), the constants $\lambda^{\text{NL}} > 0$ and $\mu^{\text{NL}} > 0$ are determined such that $\mathbb{E}[Q_\nu^{\text{NL}}(p_\nu^{\text{NL}}, \varrho_\nu^{\text{NL}})] = Q$

and $\mathbb{E}[p_\nu^{\text{NL}}] = P_{\text{avg}}$. Note that the existing mode switching scheme of [9] can be considered as a simplified special case of the proposed scheme when $P_{\text{ID},\nu}^{\text{NL}} = 1$ and $P_{\text{EH},\nu}^{\text{NL}} = 0$ (or $P_{\text{ID},\nu}^{\text{NL}'} = 1$ and $P_{\text{EH},\nu}^{\text{NL}'} = 0$).

Comparing the proposed and existing schemes, we gain the further useful insights as follows:

- From the results of (24), (28), and (36)–(38), we can make the following observations. In the proposed and existing schemes, the information/energy transmission is turned off when the channel gain is very small to save the transmit power. However, in the moderate to large range of the channel gains, the proposed and existing schemes become very different. For example, in the proposed and existing schemes, the received power is used for different purposes, similarly as discussed in Section III-C. The further insights into the transmit power allocation are given as follows. First, in the optimal dynamic power splitting scheme for the linear EH, the transmit power is allocated to maximize the amount of information transfer for the *moderate* channel gains; whereas, in the optimal dynamic power splitting scheme for the nonlinear EH, the transmit power is allocated to maximize the amount of information transfer for the *small* or *large* channel gains. Second, in the optimal mode switching scheme for the nonlinear EH, the transmit power is allocated to maximize the amount of information transfer *or* energy transfer; whereas, in the optimal dynamic power splitting scheme for the nonlinear EH, the transmit power is allocated to maximize the amount of information transfer *and* energy transfer.

V. NUMERICAL RESULTS

In this section, the performance of the proposed scheme is demonstrated through the numerical results and it is compared to that of the existing schemes of [12], [8], [9]. The R-E tradeoff performance is evaluated based on the nonlinear

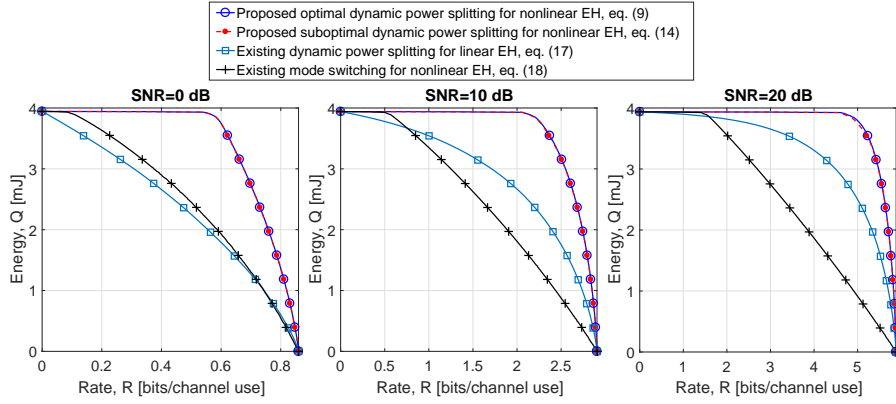


Fig. 2. R-E regions of the proposed and existing schemes for the case of CSIR.

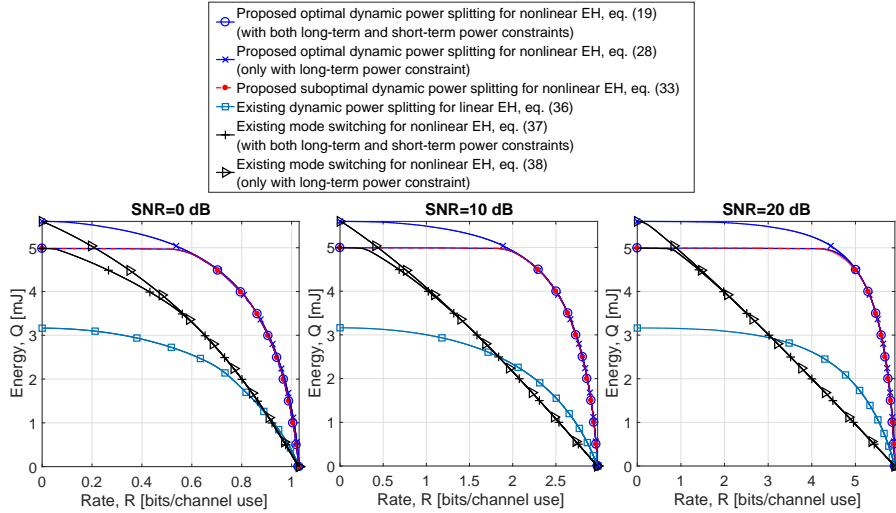


Fig. 3. R-E regions of the proposed and existing schemes for the case of CSIT.

EH model of (3). In the simulations, we set $a = 6400$ and $b = 0.003$ as in [24], [26], which were obtained based on the measurement data of [28]. The block duration is normalized to unity, i.e., $T = 1$ second. Also, we set $P = P_{\text{avg}} = 2$ W, $P_{\text{max}} = 4$ W, and $P_s = \mathbb{E}[h_\nu]P_{\text{avg}}$. The average (receive) SNR is defined as $\text{SNR} = \frac{\mathbb{E}[h_\nu]P_{\text{avg}}}{\sigma^2}$. Unless stated otherwise, the fading blocks are generated randomly according to the Rician channel model as follows: $\eta_\nu = \sqrt{\frac{\alpha}{\alpha+1}}\bar{\eta} + \sqrt{\frac{1}{\alpha+1}}\tilde{\eta}_\nu$, $\forall \nu$, where η_ν is the channel at the fading state ν . Thus, the channel power gain h_ν at that state is given by $h_\nu = |\eta_\nu|^2$. Also, α is the Rician factor, and $\bar{\eta}$ and $\tilde{\eta}_\nu \sim \mathcal{CN}(0, \sigma_h^2)$ are the line-of-sight and scattering components, respectively. We set $\alpha = 1$ and $|\bar{\eta}|^2 = \sigma_h^2 = -28$ dBW.

In Figs. 2 and 3, the R-E regions of the proposed and existing schemes are shown for the cases of CSIR and CSIT, respectively, when $\text{SNR} \in \{0, 10, 20\}$ dB. From Figs. 2 and 3, one can see that the proposed schemes significantly outperform the existing schemes in terms of the R-E tradeoff performance. For the case of CSIT, only with the long-term power constraint, the proposed optimal scheme yields the best performance. As expected from Lemma 3, the proposed suboptimal scheme provides the optimal performance in the low SNR range (e.g.,

when $\text{SNR} = 0$ dB). Interestingly, however, even in the moderate and high SNR ranges (e.g., when $\text{SNR} \in \{10, 20\}$ dB), this scheme performs very well and its performance is almost the same as the optimal performance. There exists a tradeoff between the existing schemes. In the higher rate regime, the existing dynamic power splitting scheme for the linear EH performs better than the existing mode switching scheme for the nonlinear EH. On the other hand, in the lower rate regime, the existing dynamic power splitting scheme for the linear EH is even worse than the existing mode switching scheme for the nonlinear EH due to the inaccurate or mismatched rules for power splitting and/or power allocation.

Considering the practical applications such as the Internet-of-Things (IoT) with implanted bio and/or wearable sensors, in Fig. 4, we investigate the impact of the receiver mobility on the R-E tradeoff performance. In Fig. 4, the R-E regions of the proposed and existing schemes are shown for the cases of CSIR and CSIT when $\text{SNR} = 15$ dB. In this figure, we model the channel power gain as follows: $h_\nu = 1 - e^{-\frac{a_t a_r}{(c/f_c)^2 d_\nu^2}}$, $\forall \nu$ [33], where a_t is the aperture of the transmit antenna; a_r the aperture of the receive antenna; c the speed of light; and d_ν the distance between the transmitter and the receiver. Assuming that the receiver is a small sensor, we set $a_t = 0.5$

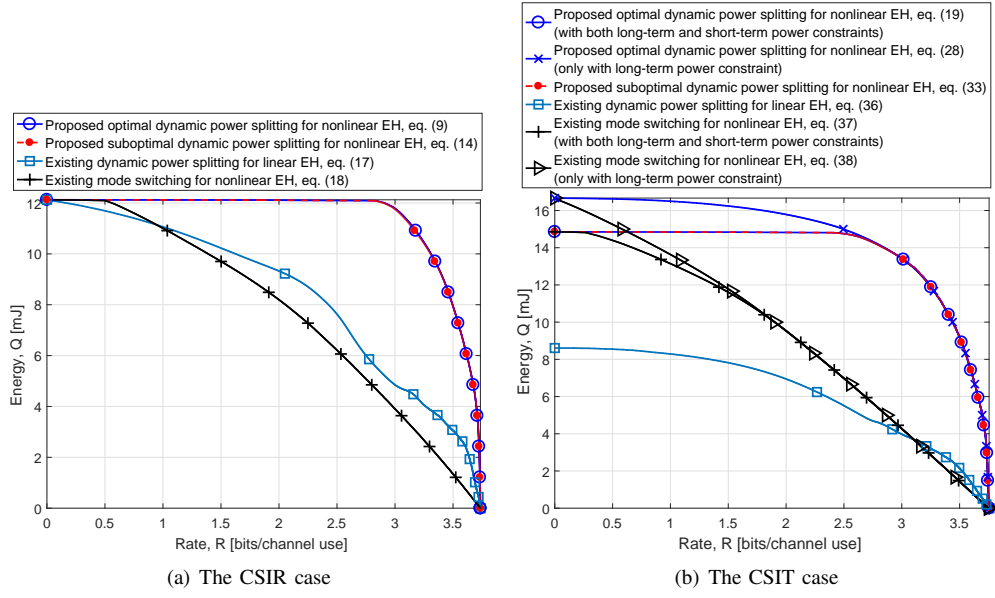


Fig. 4. R-E regions of the proposed and existing schemes with the receiver mobility when SNR = 15 dB.

m , $a_r = 0.01$ m, and $f_c = 2.4$ GHz [4]–[6]. Also, considering the mobility of the receiver, we set the distance d_ν in the current fading state ν as follows: $d_\nu = d_{\nu'} + \beta_\nu v_{\max} T$, where $d_{\nu'}$ is the distance in the previous fading state ν' ; v_{\max} the maximum speed; and β_ν the parameter accounting for the directionality. We set the initial distance to 15 m and we select β_ν randomly over the range $[-1, 1]$. Also, we set $v_{\max} = 0.1$ m/s. From Fig. 4, it can be seen that in the scenario of the receiver mobility, the proposed schemes are much better than the existing schemes, which clearly shows the significant advantages of the proposed schemes over the existing schemes in the practical applications.

VI. CONCLUSION

In this paper, we studied the dynamic power splitting for the SWIPT system with nonlinear EH in the ergodic fading channel in the sense of maximizing the R-E region. First, we developed the optimal and suboptimal dynamic power splitting scheme for the cases of CSIR. Then we developed the optimal and suboptimal schemes for case of CSIT where the feedback link between the transmitter and the receiver exists. Comparing the proposed schemes to the existing schemes, the useful insights were obtained. The numerical results showed that the proposed schemes considerably outperformed the existing schemes and the proposed suboptimal scheme performed very close to the optimal scheme.

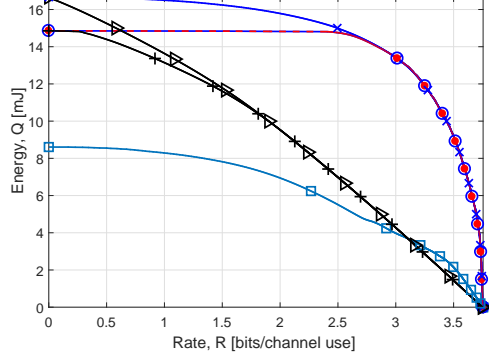
APPENDIX A PROOFS OF LEMMAS 1 AND 4

In this proof, we first prove the result of Lemma 4. Then we prove the result of Lemma 1.

A. Proof of Lemma 4

Let h_k denote the channel power gain at the k th block, $k = 1, \dots, N$. Also, let $\{P_{x,k}, \rho_{x,k}\}$ and $\{P_{y,k}, \rho_{y,k}\}$ denote the

- Proposed optimal dynamic power splitting for nonlinear EH, eq. (19) (with both long-term and short-term power constraints)
- Proposed optimal dynamic power splitting for nonlinear EH, eq. (28) (only with long-term power constraint)
- Proposed suboptimal dynamic power splitting for nonlinear EH, eq. (33)
- Existing dynamic power splitting for linear EH, eq. (36)
- × Existing mode switching for nonlinear EH, eq. (37) (with both long-term and short-term power constraints)
- × Existing mode switching for nonlinear EH, eq. (38) (only with long-term power constraint)



solutions to (P2) when $(Q, P_{\text{avg}}) = (Q_x, \bar{P}_x)$ and $(Q, P_{\text{avg}}) = (Q_y, \bar{P}_y)$, respectively. Taking time-sharing between these two solutions, we can obtain a feasible solution $\{P_{z,k}, \rho_{z,k}\}$ to (P2) as follows:

$$(P_{z,k}, \rho_{z,k}) = \begin{cases} (P_{x,k}, \rho_{x,k}), & k = 1, \dots, \theta N \\ (P_{y,k}, \rho_{y,k}), & k = \theta N + 1, \dots, N \end{cases} \quad (\text{A.1})$$

where $0 \leq \theta \leq 1$. Due to the law of large numbers, as $N \rightarrow \infty$, we have $\frac{1}{N} \sum_{k=1}^N R_k(P_{j,k}, \rho_{j,k}) \rightarrow \mathbb{E}[R_\nu(P_{j,\nu}, \rho_{j,\nu})]$, $\frac{1}{N} \sum_{k=1}^N Q_k^{\text{NL}}(P_{j,k}, \rho_{j,k}) \rightarrow \mathbb{E}[Q_\nu^{\text{NL}}(P_{j,\nu}, \rho_{j,\nu})]$, and $\frac{1}{N} \sum_{k=1}^N P_{j,k} \rightarrow \mathbb{E}[P_{j,\nu}]$ for $j \in \{x, y, z\}$, where $R_k(\cdot)$ and $Q_k^{\text{NL}}(\cdot)$ are given by (1) and (3), respectively, with h_ν replaced by h_k . Therefore, from (A.1), it follows that $\frac{1}{N} \sum_{k=1}^N R_k(P_{z,k}, \rho_{z,k}) = \frac{\theta}{N} \sum_{k=1}^N R_k(P_{x,k}, \rho_{x,k}) + \frac{1-\theta}{N} \sum_{k=1}^N R_k(P_{y,k}, \rho_{y,k}) \rightarrow \theta \mathbb{E}[R_\nu(P_{x,\nu}, \rho_{x,\nu})] + (1-\theta) \mathbb{E}[R_\nu(P_{y,\nu}, \rho_{y,\nu})]$ for any $0 \leq \theta \leq 1$. Similarly, $\frac{1}{N} \sum_{k=1}^N P_{z,k} \rightarrow \theta \mathbb{E}[P_{x,\nu}] + (1-\theta) \mathbb{E}[P_{y,\nu}] \leq \theta \bar{P}_x + (1-\theta) \bar{P}_y$ and $\frac{1}{N} \sum_{k=1}^N Q_k^{\text{NL}}(P_{z,k}, \rho_{z,k}) \rightarrow \theta \mathbb{E}[Q_\nu^{\text{NL}}(P_{x,\nu}, \rho_{x,\nu})] + (1-\theta) \mathbb{E}[Q_\nu^{\text{NL}}(P_{y,\nu}, \rho_{y,\nu})] \geq \theta Q_x + (1-\theta) Q_y$. Thus, (P2) satisfies the time-sharing condition.

B. Proof of Lemma 1

Following the above procedures with $P_{j,k} = P$, $\forall k, \forall j \in \{x, y, z\}$, it can be shown that (P1) satisfies the time-sharing condition.

APPENDIX B PROOF OF THEOREM 1

The Lagrange dual function for (P1) is given by [31]

$$\mathcal{D}(\lambda) = \max_{0 \leq \rho_\nu \leq 1, \forall \nu} \left\{ \mathbb{E}[R_\nu(P, \rho_\nu)] + \lambda (\mathbb{E}[Q_\nu^{\text{NL}}(P, \rho_\nu)] - Q) \right\} \quad (\text{B.1})$$

where λ is the dual variable associated with the average harvested energy constraint of (6b). To obtain the solution to (P2), in the following, we first determine the optimal ρ_ν by solving (B.1) given the dual variable λ . Then we determine the optimal λ .

A. Optimal Power Splitting Ratio Given the Dual Variable

Given λ , the problem of (B.1) can be divided into several subproblems, each for one particular fading state ν , as follows:

$$\max_{0 \leq \rho_\nu \leq 1} \mathcal{L}_\nu(\rho_\nu) \quad (\text{B.2})$$

where $\mathcal{L}_\nu(\rho_\nu) = R_\nu(P, \rho_\nu) + \lambda Q_\nu^{\text{NL}}(P, \rho_\nu)$. Because the optimization of (B.2) is nonconvex, the solution needs to be found case by case. To this end, we exploit the Karush-Kuhn-Tucker (KKT) optimality conditions for (B.2), which are given by [31]

$$\frac{\partial \mathcal{L}_\nu}{\partial \rho_\nu} = \begin{cases} \leq 0, & \text{if } \rho_\nu^* = 0 \\ \geq 0, & \text{if } \rho_\nu^* = 1 \\ = 0, & \text{if } 0 < \rho_\nu^* < 1 \end{cases} \quad (\text{B.3})$$

where ρ_ν^* denotes the solution to (B.2). Also, $\frac{\partial \mathcal{L}_\nu}{\partial \rho_\nu} = \lambda \frac{P_\nu T a h_\nu P}{1 - \Omega} \Psi_\nu(P, \rho_\nu) (1 - \Psi_\nu(P, \rho_\nu)) - \frac{h_\nu P}{((1 - \rho_\nu) h_\nu P + \sigma^2)}$.

First, we consider the case when $\gamma(h_\nu) \geq \frac{\lambda}{4}$ to derive the solution in the Case 1. The function $\Psi_\nu(P, \rho_\nu) (1 - \Psi_\nu(P, \rho_\nu))$ has its peak value of $\frac{1}{4}$ at the inflection point $\rho_\nu = \min\left\{\frac{b}{h_\nu P}, 1\right\}$. Thus, it follows that if $\left.\frac{\partial \mathcal{L}_\nu}{\partial \rho_\nu}\right|_{\rho_\nu=\min\left\{\frac{b}{h_\nu P}, 1\right\}} \leq 0$, or equivalently, $\gamma(h_\nu) \geq \frac{\lambda}{4}$, then $\left.\frac{\partial \mathcal{L}_\nu}{\partial \rho_\nu}\right|_{\rho_\nu=\min\left\{\frac{b}{h_\nu P}, 1\right\}} \leq 0$ for all $0 \leq \rho_\nu \leq 1$. Thus, from (B.3), we have $\rho_\nu^* = 0$ when $\gamma(h_\nu) \geq \frac{\lambda}{4}$, which corresponds to the result of (9) for the Case 1.

Next, we consider the case when $\gamma(h_\nu) < \frac{\lambda}{4}$ to derive the solutions in the Cases 2–5. From (B.3), we have

$$\lambda f(0) \leq g(h_\nu), \quad \text{if } \rho_\nu^* = 0 \quad (\text{B.4})$$

$$\lambda f(h_\nu) \geq g(0), \quad \text{if } \rho_\nu^* = 1. \quad (\text{B.5})$$

Also, the value of $0 < \rho_\nu^* < 1$ is given by the root of the equation $\frac{\partial \mathcal{L}_\nu}{\partial \rho_\nu} = 0$, or equivalently, the equation of (12). In general, this equation has two roots: one is the local minimum located in the range $\left[0, \frac{b}{h_\nu P}\right)$ and the other is the local maximum located in the range $\left(\frac{b}{h_\nu P}, \infty\right)$. Let $\rho_{o,\nu}$ denote the local maximum. The solution satisfying $\frac{\partial \mathcal{L}_\nu}{\partial \rho_\nu} = 0$ is given by $\rho_\nu^* = \rho_{o,\nu}$. It follows from (B.3) that if $\left.\frac{\partial \mathcal{L}_\nu}{\partial \rho_\nu}\right|_{\rho_\nu=1} < 0$, or equivalently, $\lambda f(h_\nu) < g(0)$, then the solution ρ_ν^* can be found by solving the equation of (12) over $\left(\frac{b}{h_\nu P}, 1\right)$. Thus, we have

$$\lambda f(h_\nu) < g(0), \quad \text{if } 0 < \rho_\nu^* < 1. \quad (\text{B.6})$$

As can be seen from (B.4)–(B.6), when $\gamma(h_\nu) < \frac{\lambda^{\text{NL}}}{4}$, the optimal conditions in (B.3) depend on the channel power gain h_ν through the functions $f(\cdot)$ and $g(\cdot)$. In the following, we derive the solution to (B.2) for the following four possible cases.

i) $\lambda f(0) \leq g(h_\nu)$ and $\lambda f(h_\nu) < g(0)$: In this case, both the conditions (B.4) and (B.6) are satisfied. Thus, the solution can be either $\rho_\nu^* = 0$ or $\rho_\nu^* = \rho_{o,\nu}$. To obtain the solution, we need to compare the two objective values: $\mathcal{L}_\nu(0)$ and $\mathcal{L}_\nu(\rho_{o,\nu})$. If $\mathcal{L}_\nu(\rho_{o,\nu}) > \mathcal{L}_\nu(0)$, or equivalently, $R_\nu(P, \rho_{o,\nu}) + \lambda Q_\nu^{\text{NL}}(P, \rho_{o,\nu}) > R_\nu(P, 0)$, we have $\rho_\nu^* = \rho_{o,\nu}$. Otherwise, we have $\rho_\nu^* = 0$.

ii) $\lambda f(0) \leq g(h_\nu)$ and $\lambda f(h_\nu) \geq g(0)$: In this case, both the conditions (B.4) and (B.5) are satisfied. Thus, the solution can be either $\rho_\nu^* = 0$ or $\rho_\nu^* = 1$. To obtain the solution, we need to compare the two objective values: $\mathcal{L}_\nu(0)$ and $\mathcal{L}_\nu(1)$. If $\mathcal{L}_\nu(1) > \mathcal{L}_\nu(0)$, or equivalently, $\lambda Q_\nu^{\text{NL}}(P, 1) > R_\nu(P, 0)$, we have $\rho_\nu^* = 1$. Otherwise, we have $\rho_\nu^* = 0$.

iii) $\lambda f(0) > g(h_\nu)$ and $\lambda f(h_\nu) < g(0)$: In this case, only the condition (B.6) is satisfied. Thus, we have $\rho_\nu^* = \rho_{o,\nu}$.

iv) $\lambda f(0) > g(h_\nu)$ and $\lambda f(h_\nu) \geq g(0)$: In this case, only the condition (B.5) is satisfied. Thus, we have $\rho_\nu^* = 1$.

The solutions obtained for the above four cases i)–iv) correspond to the result of (9) for the Cases 2–5, respectively.

B. Optimal Dual Variable

The optimal value of λ can be found by solving the dual problem: $\min_{\lambda \geq 0} \mathcal{D}(\lambda)$. From the KKT condition, the optimal λ can be determined to satisfy the following completeness slackness condition [31]: $\lambda (\mathbb{E}[Q_\nu^{\text{NL}}(P, \rho_\nu^*)] - Q) = 0$. If $\lambda = 0$, then $\rho_\nu^* = 0$ for $\forall \nu$, which is infeasible for (P1). It thus must be $\lambda > 0$, meaning that the average harvested energy constraint of (6b) must be satisfied with equality. Therefore, the optimal λ is chosen to satisfy $\mathbb{E}[Q_\nu^{\text{NL}}(P, \rho_\nu^*)] = Q$. Let λ^{NL} denote the optimal dual variable. Then, substituting λ^{NL} into ρ_ν^* , and changing the terms ρ_ν^* and $\rho_{o,\nu}$ to ρ_ν^{NL} and $\rho_{o,\nu}^{\text{NL}}$, respectively, the optimal solution to (P1) can be expressed as in Theorem 1.

APPENDIX C PROOF OF THEOREM 3

In this proof, we first transform (P2) into a more tractable form. Then we derive the optimal solution by solving the transformed problem.

A. Problem Transformation

Let us define the following new variables: $\rho_\nu P_\nu = P_{\text{EH},\nu}$ and $(1 - \rho_\nu)P_\nu = P_{\text{ID},\nu}$, $\forall \nu$, which denote the power allocation for ID and EH, respectively. Then the problem (P2) can be equivalently written in the following form:

$$(P3) : \max_{\substack{0 \leq P_{\text{ID},\nu} + P_{\text{EH},\nu} \leq P_{\text{max}}, \forall \nu, \\ P_{\text{ID},\nu} \geq 0, P_{\text{EH},\nu} \geq 0, \forall \nu}} \mathbb{E}[R_\nu(P_{\text{ID},\nu}, 0)] \quad (\text{C.1a})$$

$$\text{s.t.} \quad \mathbb{E}[Q_\nu^{\text{NL}}(P_{\text{EH},\nu}, 1)] \geq Q, \quad (\text{C.1b})$$

$$\mathbb{E}[P_{\text{ID},\nu} + P_{\text{EH},\nu}] \leq P_{\text{avg}}. \quad (\text{C.1c})$$

Let $(P_{\text{ID},\nu}^{\text{NL}}, P_{\text{EH},\nu}^{\text{NL}})$ denote the optimal solution to the above problem (P3). Then, from $(P_{\text{ID},\nu}^{\text{NL}}, P_{\text{EH},\nu}^{\text{NL}})$, the optimal solution $(\rho_\nu^{\text{NL}}, \rho_{o,\nu}^{\text{NL}})$ to (P2) can be obtained by (24). Thus, in the following, we focus on deriving the solution to (P3).

B. Optimal Power Allocation for ID and EH

The Lagrange dual function for (P3) is given by

$$\begin{aligned} \mathcal{D}(\lambda, \mu) = & \max_{\substack{0 \leq P_{ID,\nu} + P_{EH,\nu} \leq P_{\max}, \forall \nu, \\ P_{ID,\nu} \geq 0, P_{EH,\nu} \geq 0, \forall \nu}} \left\{ \mathbb{E}[R_\nu(P_{ID,\nu}, 0)] + \lambda \right. \\ & \left. \times (\mathbb{E}[Q_\nu^{\text{NL}}(P_{EH,\nu}, 1)] - Q) + \mu (P_{\text{avg}} - \mathbb{E}[P_{ID,\nu} + P_{EH,\nu}]) \right\} \end{aligned} \quad (\text{C.2})$$

where λ and μ denote the dual variables associated with the constraints of (C.1b) and (C.1c), respectively. Similarly as in the case of (P1), it can be shown that the optimal dual variables λ^{NL} and μ^{NL} must be positive, i.e., $\lambda^{\text{NL}} > 0$ and $\mu^{\text{NL}} > 0$, meaning that both the constraints of (8b) and (8c) with equality, i.e., $\mathbb{E}[Q_\nu^{\text{NL}}(P_{EH,\nu}^*, 1)] = Q$ and $\mathbb{E}[P_{ID,\nu}^* + P_{EH,\nu}^*] = P_{\text{avg}}$, respectively, where $(P_{ID,\nu}^*, P_{EH,\nu}^*)$ denotes the solution to (C.2). Thus, in the following, we focus on deriving the solution $(P_{ID,\nu}^*, P_{EH,\nu}^*)$ to (C.2) given the dual variables λ and μ .

Given λ and μ , the problem of (C.2) can be decoupled into several subproblems, each for one particular fading state ν , as follows:

$$\max_{\substack{0 \leq P_{ID,\nu} + P_{EH,\nu} \leq P_{\max}, \\ P_{ID,\nu} \geq 0, P_{EH,\nu} \geq 0}} \mathcal{L}_\nu(P_{ID,\nu}, P_{EH,\nu}) \quad (\text{C.3})$$

where $\mathcal{L}_\nu(P_{ID,\nu}, P_{EH,\nu}) = R_\nu(P_{ID,\nu}, 0) - \mu P_{ID,\nu} + \lambda Q_\nu^{\text{NL}}(P_{EH,\nu}, 1) - \mu P_{EH,\nu}$. The above problem (C.3) is solved as follows: first, the optimal $P_{ID,\nu}$ is determined (as a function of $P_{EH,\nu}$), and then, the optimal $P_{EH,\nu}$ is determined. Specifically, in (C.3), the solution $P_{ID,\nu}^*$ is given by the well-known water-filling power allocation: $P_{ID,\nu}^* = \min \left\{ \max \left\{ \frac{1}{\mu} - \frac{\sigma^2}{h_\nu}, 0 \right\}, P_{\max} - P_{EH,\nu} \right\}$ [15, Ch. 5.3.3]. Substituting this into (C.3), the optimization of (C.3) reduces to the optimization only over the variable $P_{EH,\nu}$, from which the solution $P_{EH,\nu}^*$ can be obtained. The details are given below.

1) *Optimal Power Allocation for EH When $h_\nu \leq \mu\sigma^2$:* When $h_\nu \leq \mu\sigma^2$, we have $P_{ID,\nu}^* = 0$. Thus, the optimization of (C.3) becomes:

$$\max_{0 \leq P_{EH,\nu} \leq P_{\max}} \lambda Q_\nu^{\text{NL}}(P_{EH,\nu}, 1) - \mu P_{EH,\nu}. \quad (\text{C.4})$$

The solution to the above problem (C.4) can be obtained by following the similar procedures in [9, Appendix B] (the detailed proof is omitted due to the space limit). Consequently, it is given by $P_{EH,\nu}^* = [P_{EH,\nu}^A]_{0}^{P_{\max}}$, where $[P_{EH,\nu}^A]_{P_{\text{low}}}^{P_{\text{up}}}$ is given by (20).

2) *Optimal Power Allocation for EH When $h_\nu > \mu\sigma^2$:* When $h_\nu > \mu\sigma^2$, it follows that $P_{ID,\nu}^* = \min \left\{ \frac{1}{\mu} - \frac{\sigma^2}{h_\nu}, P_{\max} - P_{EH,\nu} \right\}$. Thus, we have the following two sub-cases:

2-i) $0 \leq P_{EH,\nu} \leq P_{\text{th},\nu}$: In this sub-case, we have $\frac{1}{\mu} - \frac{\sigma^2}{h_\nu} \leq P_{\max} - P_{EH,\nu}$, and thus, $P_{ID,\nu}^* = \frac{1}{\mu} - \frac{\sigma^2}{h_\nu}$. Substituting this into (C.3) and dropping the constant term, the optimization of (C.3) becomes:

$$\max_{0 \leq P_{EH,\nu} \leq P_{\text{th},\nu}} \lambda Q_\nu^{\text{NL}}(P_{EH,\nu}, 1) - \mu P_{EH,\nu}. \quad (\text{C.5})$$

Similarly as in (C.4), the solution to (C.5) is given by $P_{EH,\nu}^* = [P_{EH,\nu}^A]_{0}^{P_{\text{th},\nu}}$.

2-ii) $P_{\text{th},\nu} < P_{EH,\nu} \leq P_{\max}$: In this sub-case, we have $\frac{1}{\mu} - \frac{\sigma^2}{h_\nu} \leq P_{\max} - P_{EH,\nu}$, and thus, $P_{ID,\nu}^* = P_{\max} - P_{EH,\nu}$. Substituting this into (C.3) and dropping the constant term, the optimization of (C.3) becomes:

$$\max_{0 \leq P_{EH,\nu} \leq P_{\text{th},\nu}} R_\nu(P_{\max} - P_{EH,\nu}, 0) + \lambda Q_\nu^{\text{NL}}(P_{EH,\nu}, 1). \quad (\text{C.6})$$

Following the similar procedures in Appendix B, it can be shown that the solution to (C.6) is given by $P_{EH,\nu}^* = [P_{EH,\nu}^B]_{P_{\text{th},\nu}}^{P_{\max}}$, where $[P_{EH,\nu}^B]_{P_{\text{low}}}^{P_{\text{up}}}$ is given by (22).

To obtain the solution when $h_\nu > \mu\sigma^2$, we need to compare the two objective values of (C.3) for the above two sub-cases: one is given by $\mathcal{L}_\nu \left(\frac{1}{\mu} - \frac{\sigma^2}{h_\nu}, [P_{EH,\nu}^A]_{0}^{P_{\text{th},\nu}} \right) = \log_2 \left(\frac{h_\nu}{\lambda\sigma^2} \right) + \frac{\lambda\sigma^2}{h_\nu} - 1 + \lambda Q_\nu^{\text{NL}}(P_{EH,\nu}, 1) - \mu \cdot [P_{EH,\nu}^A]_{0}^{P_{\text{th},\nu}}$ and the other is given by $\mathcal{L}_\nu \left(P_{\max} - [P_{EH,\nu}^B]_{P_{\text{th},\nu}}^{P_{\max}}, [P_{EH,\nu}^B]_{P_{\text{th},\nu}}^{P_{\max}} \right) = R_\nu(P_{\max} - P_{EH,\nu}, 0) + \lambda Q_\nu^{\text{NL}}(P_{EH,\nu}, 1) - \mu P_{\max}$. If the former is larger than the latter, we have $(P_{ID,\nu}^*, P_{EH,\nu}^*) = \left(\frac{1}{\mu} - \frac{\sigma^2}{h_\nu}, [P_{EH,\nu}^A]_{0}^{P_{\text{th},\nu}} \right)$. Otherwise, we have $(P_{ID,\nu}^*, P_{EH,\nu}^*) = \left(P_{\max} - [P_{EH,\nu}^B]_{P_{\text{th},\nu}}^{P_{\max}}, [P_{EH,\nu}^B]_{P_{\text{th},\nu}}^{P_{\max}} \right)$.

REFERENCES

- [1] X. Lu, P. Wang, D. Niyato, D. I. Kim, and Z. Han, "Wireless networks with RF energy harvesting: A contemporary survey," *IEEE Commun. Surv. Tuts.*, vol. 17, no. 2, pp. 757–789, Second Quart. 2015.
- [2] R. Zhang and C. K. Ho, "MIMO broadcasting for simultaneous wireless information and power transfer," *IEEE Trans. Wireless Commun.*, vol. 12, no. 5, pp. 1989–2001, May 2013.
- [3] X. Zhou, R. Zhang, and C. K. Ho, "Wireless information and power transfer: Architecture design and rate-energy tradeoff," *IEEE Trans. Commun.*, vol. 61, no. 11, pp. 4753–4767, Nov. 2013.
- [4] I.-M. Kim and D. I. Kim, "Wireless information and power transfer: Rate-energy tradeoff for equi-probable arbitrary-shaped discrete inputs," *IEEE Trans. Wireless Commun.*, vol. 15, no. 6, pp. 4393–4407, Jun. 2016.
- [5] I.-M. Kim, D. I. Kim, and J.-M. Kang, "Rate-energy tradeoff and decoding error probability-energy tradeoff for SWIPT in finite codelength," *IEEE Trans. Wireless Commun.*, vol. 16, no. 12, pp. 8220–8234, Dec. 2017.
- [6] J.-M. Kang, I.-M. Kim, and D. I. Kim, "Wireless information and power transfer: Rate-energy tradeoff for nonlinear energy harvesting," *IEEE Trans. Wireless Commun.*, vol. 17, no. 3, pp. 1966–1981, Mar. 2018.
- [7] J.-M. Kang, I.-M. Kim, and D. I. Kim, "Joint Tx power allocation and Rx power splitting for SWIPT system with multiple nonlinear energy harvesting circuits," *arXiv:1804.00387*, 2018.
- [8] J.-M. Kang, I.-M. Kim, and D. I. Kim, "Mode switching for SWIPT over fading channel with nonlinear energy harvesting," *IEEE Wireless Commun. Lett.*, vol. 6, no. 5, pp. 678–680, Oct. 2017.
- [9] J.-M. Kang, I.-M. Kim, and D. I. Kim, "Joint optimal mode switching and power adaptation for nonlinear energy harvesting SWIPT system over fading channel," accepted for publication, *IEEE Trans. Commun.*, 2017.
- [10] S. Lee, L. Liu, and R. Zhang, "Collaborative wireless energy and information transfer in interference channel," *IEEE Trans. Wireless Commun.*, vol. 14, no. 1, pp. 545–557, Jan. 2015.
- [11] H. Xing, L. Liu, and R. Zhang, "Secrecy wireless information and power transfer in fading wiretap channel," *IEEE Trans. Veh. Technol.*, vol. 65, no. 1, pp. 180–190, Jan. 2016.
- [12] L. Liu, R. Zhang, and K.-C. Chua, "Wireless information transfer with opportunistic energy harvesting," *IEEE Trans. Wireless Communications*, vol. 12, no. 1, pp. 288–300, Jan. 2013.
- [13] W. Lu, Y. Gong, J. Wu, H. Peng, and J. Hua, "Simultaneous wireless information and power transfer based on joint subcarrier and power allocation in OFDM systems," *IEEE Access*, vol. 5, pp. 2763–2770, 2017.

- [14] L. Liu, R. Zhang, and K. C. Chua, "Wireless information and power transfer: A dynamic power splitting approach," *IEEE Trans. Commun.*, vol. 61, no. 9, pp. 3990–4001, Sep. 2013.
- [15] D. N. C. Tse and P. Viswanath, *Fundamentals of Wireless Communications*. Cambridge, U.K.: Cambridge Univ. Press, 2005.
- [16] B. Clerckx, R. Zhang, R. Schober, D. W. K. Ng, D. I. Kim, and H. V. Poor, "Fundamentals of wireless information and power transfer: From RF energy harvester models to signal and system designs," *arXiv:1803.07123*, 2018.
- [17] Y. Zeng, B. Clerckx, and R. Zhang, "Communications and signals design for wireless power transmission," *IEEE Trans. Commun.*, vol. 65, no. 5, pp. 2264–2290, May 2017.
- [18] B. Clerckx and E. Bayguzina, "Waveform design for wireless power transfer," *IEEE Trans. Signal Process.*, vol. 64, no. 23, pp. 6313–6328, Dec. 2016.
- [19] B. Clerckx, "Wireless information and power transfer: Nonlinearity, waveform design and rate-energy tradeoff," *IEEE Trans. Signal Process.*, vol. 66, No. 4, pp. 847–862, Feb. 2018.
- [20] B. Clerckx, Z. B. Zawawi, and K. Huang "Wirelessly powered backscatter communications: Waveform design and SNR-energy tradeoff," *IEEE Commun. Lett.*, vol. 21, no. 10, pp. 2234–2237, Oct. 2017.
- [21] M. Varasteh, B. Rassouli, and B. Clerckx, "Wireless information and power transfer over an AWGN channel: Nonlinearity and asymmetric gaussian signaling," *arXiv:1705.06350*, 2017.
- [22] D. I. Kim, J. H. Moon, and J. J. Park, "New SWIPT using PAPR: How it works," *IEEE Wireless Commun. Lett.*, vol. 5, no. 6, pp. 672–675, Dec. 2016.
- [23] X. Xu, A. Ozcelikkale, T. McKelvey, and M. Viberg, "Simultaneous information and power transfer under a non-linear RF energy harvesting model," in *Proc. IEEE ICC Workshops*, Paris, France, 2017, pp. 179–184.
- [24] E. Boshkovska, D. W. K. Ng, N. Zlatanov, and R. Schober, "Practical nonlinear energy harvesting model and resource allocation for SWIPT systems," *IEEE Commun. Lett.*, vol. 19, no. 12, pp. 2082–2085, Dec. 2015.
- [25] E. Boshkovska, D. W. K. Ng, N. Zlatanov, A. Koelpin, and R. Schober, "Robust resource allocation for MIMO wireless powered communication networks with non-linear EH model," *IEEE Trans. Commun.*, vol. 65, no. 5, pp. 1984–1999, May 2017.
- [26] E. Boshkovska, N. Zlatanov, L. Dai, D. W. K. Ng, and R. Schober, "Secure SWIPT networks based on a non-linear energy harvesting model," in *Proc. IEEE Wireless Commun. and Netw. Conf.*, San Francisco, CA, USA, Mar. 2017, pp. 1–6.
- [27] C. Valenta and G. Durgin, "Harvesting wireless power: Survey of energy harvester conversion efficiency in far-field wireless power transfer systems," *IEEE Microw. Mag.*, vol. 15, no. 4, pp. 108–120, Jun. 2014.
- [28] T. Le, K. Mayaram, and T. Fiez, "Efficient far-field radio frequency energy harvesting for passively powered sensor networks," *IEEE J. Solid-State Circuits*, vol. 43, no. 5, pp. 1287–1302, May 2008.
- [29] J. Guo and X. Zhu, "An improved analytical model for RF-DC conversion efficiency in microwave rectifiers," in *Proc. IEEE MTT-S Int. Microw. Symp. Dig.*, Montreal, QC, Canada, 2012, pp. 1–3.
- [30] W. Yu and R. Lui, "Dual methods for nonconvex spectrum optimization of multicarrier systems," *IEEE Trans. Commun.*, vol. 54, no. 7, pp. 1310–1322, Jul. 2006.
- [31] S. Boyd and L. Vandenberghe, *Convex Optimization*. Cambridge, U.K.: Cambridge Univ. Press, 2009.
- [32] (2010). Federal Communications Commission: Rules and Regulations. [Online]. Available: <http://www.fcc.gov/oet/info/rules/>
- [33] K. Huang and X. Zhou, "Cutting the last wires for mobile communications by microwave power transfer," *IEEE Commun. Mag.*, vol. 53, no. 6, pp. 86–93, Jun. 2015.